

Dear Author

Here are the proofs of your article.

- You can submit your corrections **online**, via **e-mail** or by **fax**.
- For **online** submission please insert your corrections in the online correction form. Always indicate the line number to which the correction refers.
- You can also insert your corrections in the proof PDF and **email** the annotated PDF.
- For **fax** submission, please ensure that your corrections are clearly legible. Use a fine black pen and write the correction in the margin, not too close to the edge of the page.
- Remember to note the **journal title**, **article number**, and **your name** when sending your response via e-mail or fax.
- **Check** the metadata sheet to make sure that the header information, especially author names and the corresponding affiliations are correctly shown.
- **Check** the questions that may have arisen during copy editing and insert your answers/corrections.
- **Check** that the text is complete and that all figures, tables and their legends are included. Also check the accuracy of special characters, equations, and electronic supplementary material if applicable. If necessary refer to the *Edited manuscript*.
- The publication of inaccurate data such as dosages and units can have serious consequences. Please take particular care that all such details are correct.
- Please **do not** make changes that involve only matters of style. We have generally introduced forms that follow the journal's style.
- Substantial changes in content, e.g., new results, corrected values, title and authorship are not allowed without the approval of the responsible editor. In such a case, please contact the Editorial Office and return his/her consent together with the proof.
- If we do not receive your corrections **within 48 hours**, we will send you a reminder.
- Your article will be published **Online First** approximately one week after receipt of your corrected proofs. This is the **official first publication** citable with the DOI. **Further changes are, therefore, not possible.**
- The **printed version** will follow in a forthcoming issue.

Please note

After online publication, subscribers (personal/institutional) to this journal will have access to the complete article via the DOI using the URL:

<http://dx.doi.org/10.1007/s00445-015-0922-2>

If you would like to know when your article has been published online, take advantage of our free alert service. For registration and further information, go to:

<http://www.link.springer.com>.

Due to the electronic nature of the procedure, the manuscript and the original figures will only be returned to you on special request. When you return your corrections, please inform us, if you would like to have these documents returned.

1	Article Title	Basaltic maar-diatreme volcanism in the lower carboniferous of the limerick basin (Southern Ireland)
2	Article Sub-Title	
3	Article Copyright - Year	Springer-Verlag Berlin Heidelberg 2015 (This will be the copyright line in the final PDF)
4	Journal Name	Bulletin of Volcanology
5		Family Name Elliott
6		Particle
7		Given Name H. A. L.
8		Suffix
9	Corresponding Author	Organization University of Southampton
10		Division Ocean and Earth Science, National Oceanography Centre, Southampton
11		Address Southampton, SO14 3ZH, UK
12		e-mail Holly.Elliott@noc.soton.ac.uk
13		Family Name Gernon
14		Particle
15		Given Name T. M.
16		Suffix
17	Author	Organization University of Southampton
18		Division Ocean and Earth Science, National Oceanography Centre, Southampton
19		Address Southampton, SO14 3ZH, UK
20		e-mail None
21		Family Name Roberts
22		Particle
23		Given Name S.
24		Suffix
25	Author	Organization University of Southampton
26		Division Ocean and Earth Science, National Oceanography Centre, Southampton
27		Address Southampton, SO14 3ZH, UK
28		e-mail None
29		Family Name Hewson
30		Particle
31		Given Name C.
32	Author	Suffix
33		Organization Teck Ireland Ltd, The Murrough
34		Division

35	Address	Wicklow, Ireland
36	e-mail	None
37	Received	8 September 2014
38	Schedule Revised	
39	Accepted	20 March 2015
40	Abstract	<p>Lead-zinc exploration drilling within the Limerick Basin (Southern Ireland) has revealed the deep internal architecture and extra-crater deposits of five alkali-basaltic maar-diatremes. These were emplaced as part of a regional north-east south-west tectonomagmatic trend during the Lower Carboniferous Period. Field relationships and textural observations suggest that the diatremes erupted into a shallow submarine environment. Limerick trace element data indicates a genetic relationship between the diatremes and extra-crater successions of the Knockroe Formation, which records multiple diatreme filling and emptying cycles. Deposition was controlled largely by bathymetry defined by the surrounding Waulsortian carbonate mounds. An initial non-diatreme forming eruption stage occurred at the water-sediment interface, with magma-water interaction prevented by high magma ascent rates. This was followed by seawater incursion and the onset of phreatomagmatic activity. Magma-water interaction generated poorly vesicular blocky clasts, although the co-occurrence of plastically deformed and highly vesicular clasts indicates that phreatomagmatic and magmatic processes were not mutually exclusive. At a later stage, the diatreme filled with a slurry of juvenile lapilli and country rock lithic clasts, homogenised by the action of debris jets. The resulting extra-crater deposits eventually emerged above sea level, so that water ingress significantly declined, and late-stage magmatic processes became dominant. These deposits, largely confined to the deep vents, incorporate high concentrations of partially sintered globular and large 'raggy' lapilli showing evidence for heat retention. Our study provides new insights into the dynamics and evolution of basaltic diatremes erupting into a shallow water (20–120 m) submarine environment.</p>
41	Keywords separated by ' - '	Raggy - Maar-diatremes - Lower Carboniferous Period
42	Foot note information	Editorial responsibility: P-S Ross

1

2 **Basaltic maar-diatreme volcanism in the lower**
 3 **carboniferous of the limerick basin (Southern Ireland)**

4 **H. A. L. Elliott¹ · T. M. Gernon¹ · S. Roberts¹ · C. Hewson²**

5 Received: 8 September 2014 / Accepted: 20 March 2015
 6 © Springer-Verlag Berlin Heidelberg 2015

7 **Abstract** Lead-zinc exploration drilling within the Limerick Basin (Southern Ireland) has revealed the deep internal architecture and extra-crater deposits of five alkali-basaltic maar-diatremes. These were emplaced as part of a regional north-east south-west tectonomagmatic trend during the Lower Carboniferous Period. Field relationships and textural observations suggest that the diatremes erupted into a shallow submarine environment. Limerick trace element data indicates a genetic relationship between the diatremes and extra-crater successions of the Knockroe Formation, which records multiple diatreme filling and emptying cycles. Deposition was controlled largely by bathymetry defined by the surrounding Waulsortian carbonate mounds. An initial non-diatreme forming eruption stage occurred at the water-sediment interface, with magma-water interaction prevented by high magma ascent rates. This was followed by seawater incursion and the onset of phreatomagmatic activity. Magma-water interaction generated poorly vesicular blocky clasts, although the co-occurrence of plastically deformed and highly vesicular clasts indicates that phreatomagmatic and magmatic processes were not mutually exclusive. At a later stage, the diatreme filled with a slurry of juvenile lapilli and country rock lithic clasts, homogenised by the action of debris

jets. The resulting extra-crater deposits eventually emerged above sea level, so that water ingress significantly declined, and late-stage magmatic processes became dominant. These deposits, largely confined to the deep vents, incorporate high concentrations of partially sintered globular and large ‘raggy’ lapilli showing evidence for heat retention. Our study provides new insights into the dynamics and evolution of basaltic diatremes erupting into a shallow water (20–120 m) submarine environment.

Keywords Raggy · Maar-diatremes · Lower Carboniferous Period

Introduction

Maar-diatremes are formed during explosive eruptions and are pre-dominantly associated with alkaline magmas including kimberlites, lamproites, and alkali basalts. Our knowledge of the behaviour of these systems is based mainly on the study of either extra-crater maar or eroded diatreme deposits. Due to their association with diamonds, kimberlites are well studied, contributing a large amount to our understanding of diatreme eruptions and their associated deposits (Mitchell 1990; Sparks et al. 2006; Walters et al. 2006; Brown et al. 2008a). In addition, maar-diatremes, although the second most common type of volcano (Lorenz 1985; Cas and Wright 1988; Lorenz 2007), tend to be eroded and poorly preserved in older sequences. In rare cases, exposures of the lower diatreme zone enables detailed investigation of the internal architecture and structure of the system (e.g., Francis (1970), Hawthorne (1975), Kurszlaukis and Lorenz (1997), Davies et al. (2008), Gernon et al. (2013), Lefebvre et al. (2013), and Mundula et al. (2013)) or preservation of extra-crater tephra deposits allow

Editorial responsibility: P-S Ross

✉ H. A. L. Elliott
 Holly.Elliott@noc.soton.ac.uk

¹ Ocean and Earth Science, National Oceanography Centre, Southampton, University of Southampton, Southampton SO14 3ZH, UK

² Teck Ireland Ltd, The Murrough, Wicklow, Ireland

Q1

Q2

62 a detailed insight into depositional processes (e.g., Fisher
63 and Waters (1970), Aranda-Gómez and Luhr (1996), Sohn
64 (1996), Gernon et al. (2009a), Calvari and Tanner (2011),
65 and Lefebvre et al. (2013)). Rarely can the maar-crater and
66 diatreme facies be studied at a single site.

67 Diatremes are irregular, cone-shaped pipes up to 2.5 km
68 deep, that erupt through country rock stratigraphy (Lorenz
69 2003; Valentine 2012). Different volcanoclastic lithofacies
70 characteristically form at different levels in the diatreme
71 (see Fig. 1); for example, the root zone consists of a series
72 of intrusions ‘feeding’ diatreme eruptions. Typically, the
73 central zone (Fig. 1) is characterised by a massive volcani-
74 clastic infill consisting of accumulated pyroclasts, crystals
75 and country-rock lithic debris trapped in the pipe (Sparks
76 et al. 2006). Diatremes are expressed at the surface as
77 maar-craters and tephra rings, typically comprising bed-
78 ded dilute pyroclastic density current (PDC) and fallout
79 deposits (Lorenz 1975). There are two plausible methods
80 for the presence of bedding in the upper diatreme. Firstly,
81 undercutting of the tephra ring by vent widening and sub-
82 sequent subsiding can form a marginal bedded facies, com-
83 monly comprising megablocks (Sparks et al. 2006; Lorenz
84 and Kurszlauskis 2007; Brown et al. 2008b; Valentine and
85 White 2012). Alternatively, the upper thinly bedded dia-
86 tremes facies may have been deposited by dilute density
87 currents in the base of the maar-crater, originating from

the same or neighbouring vents (Lorenz 1986; Lorenz and
Kurszlauskis 2007; Gernon et al. 2009a; Gernon et al. 2013;
Delpit et al. 2014).

Two key models have been proposed to explain the
emplacement of diatremes. The first, common in kimber-
litic diatreme models, involves the explosive expansion of
volatiles propagating down rising intrusions. This creates a
deep pipe resulting from a series of sub-Plinian to Plinian
eruptions (Field and Scott Smith 1999; Sparks et al. 2006;
Porritt et al. 2008). The second model involves diatreme
excavation during phreatomagmatic eruptions as magma
propagating to the surface encounters water (Lorenz 1985;
Kurszlauskis and Lorenz 1997; Kurszlauskis et al. 1998;
Lorenz and Kurszlauskis 2007; Brown et al. 2008a).

Phreatomagmatic activity can cover a range of erup-
tion styles with varying water to magma ratios. The two
main end members are briefly described here but many
eruptions lie somewhere along this scale. The first con-
sists of eruptions that involve magma explosively interact-
ing with groundwater or wet sediment, with a low water to
magma ratio of <0.3 (Wohletz and McQueen 1984; Moore
1985; Kokelaar 1986), producing gas-supported jets of
debris (cf. Lorenz et al. (2002) and McClintock and White
(2006)). These are often referred to as ‘Taaliai’ (Koke-
laar 1986; Sohn 1996) and tend to be continental eruptions
that form deep diatremes filled with volcanoclastic debris,

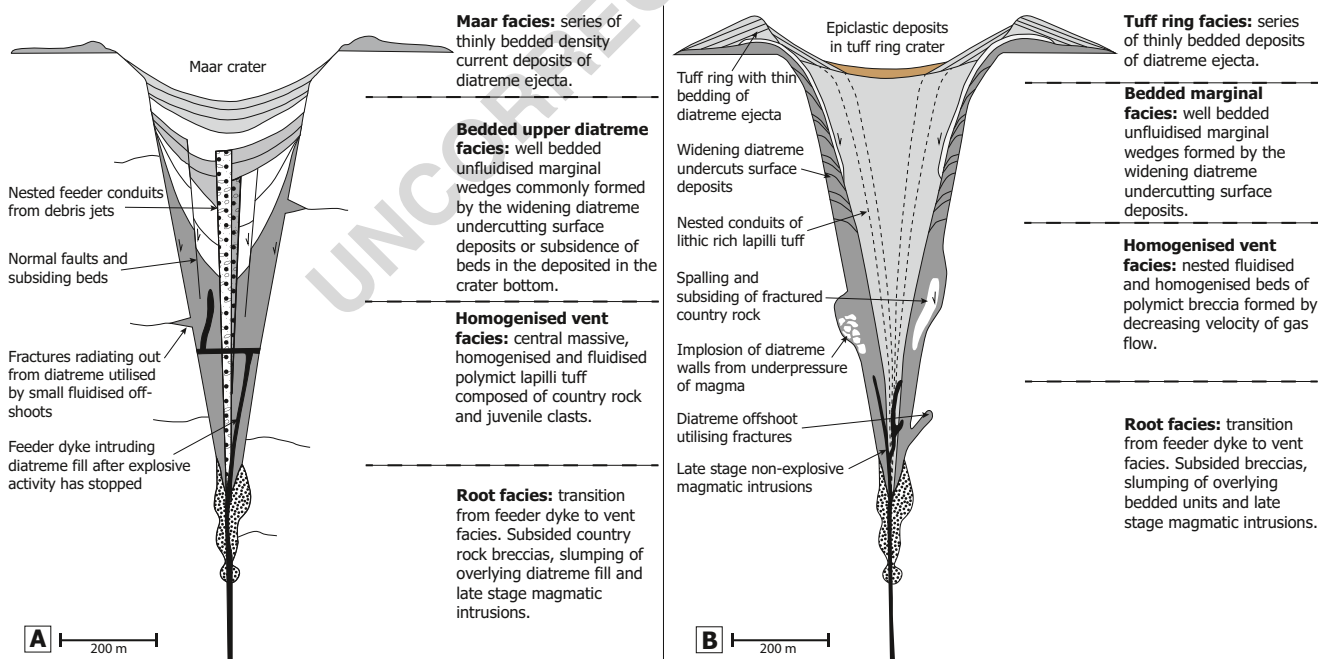


Fig. 1 **A** Schematic diagram showing the root, diatreme and maar-crater zones of a typical phreatomagmatic diatreme (modified after Lorenz and Kurszlauskis (2007)). **B** Schematic diagram showing the structure of a diatreme dominated by magmatic processes, which

typically involve multiple events of waning gas velocity due to progressive diatreme widening and/or decline in magma discharge rates (modified after Brown et al. (2008b))

114 brecciating the surrounding country rock and incorporat-
 115 ing these lithics into their maar deposits at the surface
 116 (White 1991; Lorenz et al. 2002; Valentine 2012). These
 117 maars can reach up to 5 km in diameter with craters sev-
 118 eral hundred metres deep. Maar deposits tend to be of
 119 shallow gradient and consist of well-developed beds and
 120 stratification with a high proportion of country rock clasts
 121 (Lorenz 1975; 2007; White and Ross 2011).

122 Surtseyan eruptions are at the other end of the spec-
 123 trum, involving a high water to magma ratio of ~0.3-
 124 50 (Wohletz and McQueen 1984; Kokelaar 1986). This
 125 tends to produce a funnel-shaped vent containing a par-
 126 tially fluidised and highly mobile mix of juvenile mater-
 127 ial, water and steam termed a ‘slurry’ (Kokelaar 1983;
 128 Moore 1985; Ross and White 2006). Phreatomagmatic
 129 eruptions in these conditions consist of shallow short-
 130 lived pulses of tephra jets and continuous eruptions that
 131 form due to injection of magma into this water-saturated
 132 and fluidised slurry, which is rapidly flashed-heated to
 133 steam (cf. Kokelaar (1983) and Moore (1985). Surtseyan
 134 eruptions tend to form weakly bedded tuff cones with
 135 steep flanks (White 1996; Mattsson et al. 2005; White
 136 and Ross 2011) and less than a few percent of non-
 137 juvenile clasts (White and Ross 2011). These tuff cones
 138 tend to sit on a shallowly dipping platform of volcanoclas-
 139 tic material, commonly composed of non-explosive deposits
 140 such as pillow lavas and hyaloclastites (Moore 1985)
 141 or a combination of fallout and density current deposits
 142 from both magmatic and phreatomagmatic processes
 143 (Brand and Clarke 2009).

144 A suite of alkali basaltic diatremes occurs within the
 145 Limerick Basin, part of the Irish Orefield, host to world-
 146 class lead-zinc deposits (Banks et al. 2002; Redmond
 147 2010; McCusker and Reed 2013). The Limerick Basin
 148 has recently undergone extensive mineral exploration, and
 149 borehole drilling has intersected several alkali basaltic
 150 diatremes. The drill cores, some extending to >500 metres
 151 below ground surface (mbgs), provide a unique opportunity
 152 to study deposits and the eruptive processes of basaltic
 153 diatremes.

154 This paper describes the volcanoclastic lithofacies, as
 155 observed in drill core, of two of the five identified
 156 alkali basaltic maar-diatremes from Limerick, and inter-
 157 prets these observations in the context of the magmatic
 158 and phreatomagmatic models outlined above. A model
 159 depicting a clear relationship between the diatremes and a
 160 thick sequence (up to 150 m) of extra-crater volcanoclas-
 161 tic deposits is proposed. This is a type locality for studying
 162 the deep internal structure of basaltic diatremes, with the
 163 potential to enhance our understanding of processes and
 164 interactions during explosive eruptions within a submarine
 165 environment.

Geological and geotectonic setting

166

167 The Limerick diatreme cluster is located in the western mid-
 168 lands of Ireland, immediately south of the trace of the Iape-
 169 tus suture zone (Fig.2a)—a series of major NE-SW trending
 170 faults, known to have exerted a strong influence on later
 171 tectonomagmatic activity. The diatremes erupted through a
 172 sequence of Lower Carboniferous limestones, later over-
 173 lain by pyroclastic deposits of Viséan age (Somerville et al.
 174 1992). These deposits form part of the Limerick Syncline
 175 and are offset by a series of NE-SW-trending faults. This
 176 igneous activity is part of a major phase of NE-SW trend-
 177 ing regional rifting across Europe during the Carboniferous
 178 Period (Woodcock and Strachan 2000; Wilson et al. 2004).
 179 Volcanism in Limerick was similar in style and timing to
 180 magmatic and volcanic activity in Scotland and Northern
 181 England, including East Fife (see Gernon et al. (2013))
 182 and the Whin Sill Complex (Timmerman 2004) (Fig. 2a).
 183 The extensional regime resulted from episodic N-S back
 184 arc extension in response to a Variscan subduction zone
 185 to the south, which reactivated NE-SW trending Caledo-
 186 nian basement faults (Woodcock and Strachan 2000). As a
 187 result of crustal extension, small volumes of basaltic magma
 188 ascended and fractionated extensively within the upper crust
 189 before exploiting tectonic weaknesses to reach the surface
 190 (Holland and Sanders 2009).

191 The Limerick Basin is dominated by transgressive car-
 192 bonates (Holland and Sanders 2009). The oldest country
 193 rock observed in the boreholes is the Lower Argillaceous
 194 Bioclastic Limestone (LABL), which occurs as lithic clasts
 195 within the diatreme fill. The LABL is overlain by the
 196 Waulsortian Limestone, a reef carbonate containing large
 197 cavities, with the latter thought to comprise over half the
 198 formation volume (Lees and Miller 1985; Hitzman 1995;
 199 Hitzman and Beaty 1996). Overlying the reef carbonate
 200 are the Lough Gur wackestones and cherts, the uppermost
 201 of which are interbedded with the Knockroe Formation, a
 202 series of lava flows and pyroclastic deposits (see Fig. 3)
 203 that migrate and therefore young from the west to the east
 204 (Strogen 1988; Holland and Sanders 2009). The earliest
 205 phases of Knockroe eruption are thought to be Surtseyan,
 206 initially within a submarine environment before tuff rings
 207 built up into a subaerial environment and were partially
 208 buried by subaerial basaltic lavas (Holland and Sanders
 209 2009). Using microfauna, (Somerville et al. 1992) assigned
 210 a Lower Viséan to Chadian-Arundian age (345–339 Ma)
 211 to the Knockroe Formation. Irish Waulsortian-hosted Pb-
 212 Zn deposits are precipitated in hydrothermal breccia bodies
 213 (Wilkinson et al. 2005), termed Black Matrix Breccias
 214 (BMB), which appear to have a close spatial and temporal
 215 relationship with the diatremes in Limerick. The nature of
 216 this relationship remains unclear and highly controversial.

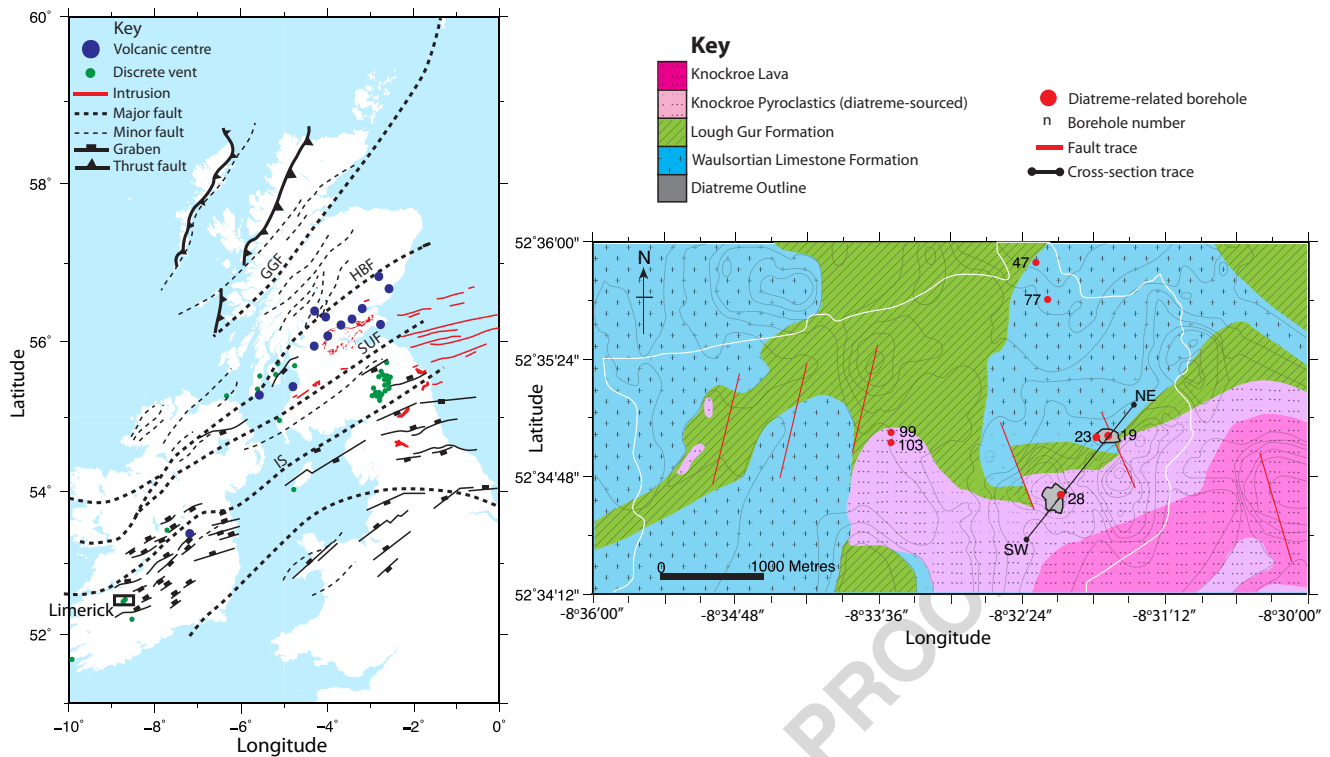


Fig. 2 **A** Regional map of the British Isles showing major NE-SW trending faults and significant volcanic centres. This tectonic and magmatic trend reflects reactivation of Caledonian basement faults by episodic N-S back arc extension related to the Variscan subduction zone to the south. *GGF*, Great Glen Fault; *HBF*, Highland Boundary Fault; *SUF* Southern Uplands Fault and *IS*, Iapetus Suture. **B** Summary geological map of the study area outlined by rectangle in (A), showing diatreme-related boreholes and outline of diatremes as resolved by magnetic surveys. Contours represent topography of study area

217 The Irish Orefield has not previously been linked to high
 218 levels of magmatic activity during the Carboniferous (Red-
 219 mond 2010; McCusker and Reed 2013).

220 **Previous studies**

221 The first detailed description of the Limerick Basin was
 222 provided by Geikie (1897) and Ashby (1939) who cor-
 223 related the diatremes they termed ‘vent-agglomerates’ to
 224 a younger Knockseefin Formation, which was deposited
 225 during the Early Asbian (Somerville et al. 1992). How-
 226 ever, textural and geochemical evidences now suggest a
 227 strong relationship with the Knockroe Formation (see Fig.
 228 5). Somerville et al. (1992) found that the Knockroe
 229 volcanoclastic rocks are interbedded with shallow water
 230 ooids and bioclastic carbonates, suggesting deposition in
 231 a shallow marine environment (Strogen et al. 1996). Stro-
 232 gen (1983,1988) determined that the Knockroe Forma-
 233 tion pyroclastic rocks generally young from west to east
 234 and identified seven breccia-filled vents across the Limer-
 235 ick Basin. Strogen (1983) showed that these vents were
 236 filled with coarse vitric-lithic tuff-breccias containing clasts

mainly of phreatomagmatic appearance (described as vitric
 237 incipiently vesicular lapilli and ash with curvi-planar
 238 surfaces and containing feldspar microphenocrysts) and
 239 lacking substantial quantities of vesicular tephra. Strogen
 240 (1983) attributed the homogeneity of the deposits, lack of
 241 bedding and presence of marginal layering to fluidisation
 242 processes during emplacement.
 243

244 **Methods and terminology**

245 **Fieldwork**

246 Although there is a little surface exposure of diatremes
 247 in the studied area of Ballyneety, Limerick (Fig. 2b),
 248 six exploration drill cores intercepted diatremes and
 249 another six intercepted volcanoclastic rocks of the Knock-
 250 roe Formation. Graphic logging recorded the characteris-
 251 tics of the volcanoclastic rocks including maximum clast
 252 length, clast composition, vesicularity, colour, angular-
 253 ity, degree of sorting, proportion of ash-grade matrix,
 254 alteration and textures. These characteristics were used

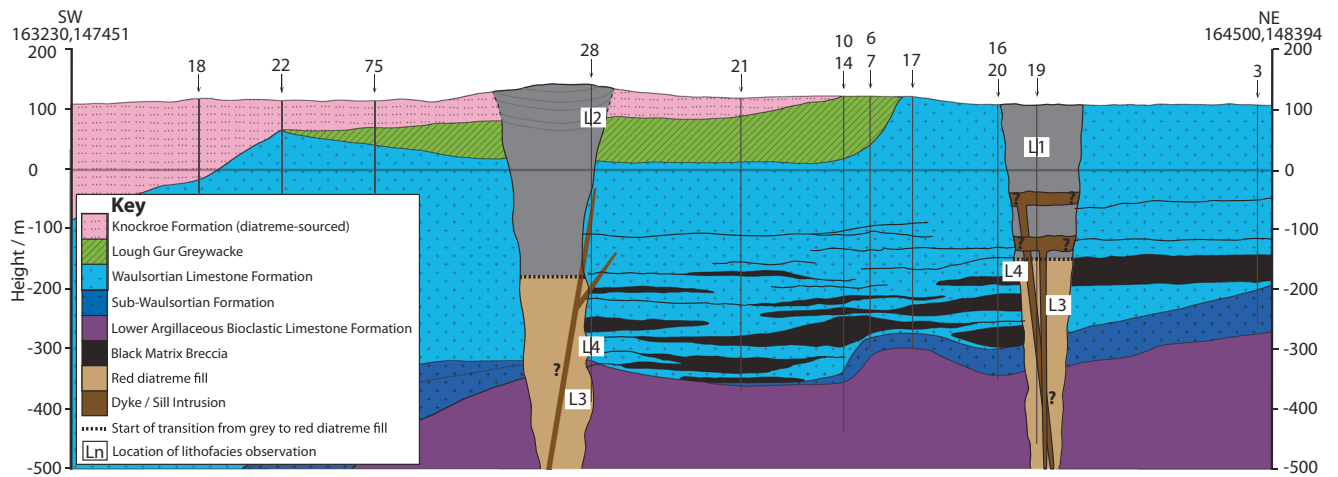


Fig. 3 Cross section showing the relationships between diatremes and the country rock sequence. The cross section shows the levels of BMB within the Waulsortian Formation and the level of major sills within the diatreme. Diatreme 28 does not intrude through the Knockroe Formation, but infills accommodation space created by the maar-crater. The

lower section of the diatremes overprinted by dolomitisation are indicated. *Boxed numbers* indicate where LFAs described in Table 2 have been observed. *Numbers* indicate the locations of boreholes drilled through the sequence (borehole data courtesy of Teck Ireland)

255 to correlate lithofacies between logs, particularly for
 256 the Knockroe Formation where beds are more laterally
 257 continuous.

258 **Laboratory work**

259 Representative samples were taken from each lithofacies and thin sections investigated using transmitted light
 260 and scanning electron microscopy (SEM). A study of
 261 vesicle size distribution was performed on the different
 262 lithofacies.
 263

264 Variations in vesicle proportions within a deposit or
 265 multiple vesicle populations within a juvenile clast can
 266 be used to elucidate magma evolution over the timescale
 267 of the eruption (Shea et al. 2010), and help to determine
 268 the eruptive style (Houghton and Wilson 1989; Ross and
 269 White 2012). Vesicularity estimates were made by man-
 270 ually digitising vesicles both in scaled photographs of
 271 thin sections and drill core. Vesicle measurements were
 272 obtained using image analysis software ImageJ and the
 273 protocols of Sahagian and Proussevitch (1998) and Shea
 274 et al. (2010). Non-vesicular lapilli are defined as 0–5 %
 275 and incipiently vesicular as 5–20 % vesicles, poorly vesic-
 276 ular ranges between 20 and 40 %, moderately vesicu-
 277 lar 40–60 %, highly vesicular ranges between 60 and
 278 80 % and >80 % vesicles is termed extremely vesicular
 279 (Houghton and Wilson 1989).

280 Trace element analysis was undertaken by solution ICP-
 281 MS on volcanic material repeatedly digested with HF and
 282 HCl and cross-referenced using several international stan-
 283 dards (including BHVO2, BIR-1, JB-1a and JA-2).

284 **Terminology**

285 Clast types and sizes were described using the protocols
 286 outlined in Fisher (1961) and White and Houghton (2006).
 287 Terms used to describe diatreme deposits follow the pro-
 288 cedure of Branney and Kokelaar (2002) and Lorenz and
 289 Kurszlaukis (2007). The term ‘autolith’ is used to describe
 290 clasts of pre-existing partially lithified diatreme fill, lapilli
 291 tuff or tuff, that have been incorporated into later deposits
 292 of similar composition (Cas et al. 2008). ‘Pelletal lapilli’
 293 is a term used to describe a core of material, for exam-
 294 ple, an autolith, phenocryst or lithic clast, that was coated
 295 in single or multiple layers of juvenile magma (Gernon
 296 et al. 2012). We follow the terminology proposed by Ingram
 297 (1964) in describing bed thickness, grain size classification
 298 after (White and Houghton 2006) and degree of vesicularity
 299 of volcanic rocks after (Houghton and Wilson 1989). Litho-
 300 facies associations are named and abbreviated based on
 301 the non-genetic scheme proposed by Branney and Kokelaar
 302 (2002).

303 **Drillcore observations and interpretations**

304 **Diatremes**

305 Boreholes drilled down the margins and centres of five
 306 diatremes in the study area provide insights into diatreme
 307 architecture. The diatremes lack surface expression because
 308 the landscape has been modified by glacial and fluvial ero-
 309 sion during the quaternary period. The diatremes appear

310 to have experienced late-stage fluid flow, forming a range
 311 of alteration products. Based on a magnetic survey, dia-
 312 treme 19 (named from intersecting borehole number) has a
 313 minimum diameter of ~170 m and a surface area of ~1.3
 314 $\times 10^4$ m², and diatreme 28 has a minimum diameter of
 315 ~240 m and a surface area of 2.6 $\times 10^4$ m² (see Fig. 2b).
 316 Measured wall angles vary between 42 and 83°, similar
 317 to the commonly observed range of 60–85° for diatremes
 318 emplaced in hard rock (Hawthorne 1975; Lorenz 2007).
 319 Assuming a maximum wall angle of 83° gives an estimated
 320 minimum volume of 5.2 $\times 10^6$ and 7.4 $\times 10^6$ m³ for dia-
 321 tremes 19 and 28, respectively. Borehole drilling ceased at
 322 < 600 m; therefore, this volume is a minimum estimate.

323 Figure 3 shows diatreme 28 with adjacent rocks of the
 324 Knockroe Formation ~40 m thick. We attribute the Knock-
 325 roe Formation to diatreme eruptions, based on their textural,
 326 petrological and geochemical similarities (see Fig. 5). The
 327 upper bedded lithofacies at the top of the diatremes, adja-
 328 cent to the extra-crater Knockroe deposits (see Fig. 3),

329 has most likely formed by debris currents, remobilisation
 330 of maar material and fallout from the water column,
 331 gradually filling up accommodation space within the maar-
 332 crater. Analogous crater deposition has been described by
 333 Lorenz (1986), Lorenz and Kurszlauskis (2007), Gernon
 334 et al. (2009a), Gernon et al. (2013) and Delpit et al. (2014).
 335 Diatreme 28 has experienced partial erosion of the extra-
 336 crater sequences; however, the entirety of the maar deposits
 337 surrounding diatreme 19 has been removed. If the same
 338 upper bedded deposits observed at the top of diatreme 28
 339 were also originally deposited in diatreme 19, a minimum
 340 of between 80 and 100 m has been eroded from the upper
 341 diatreme, excluding the height of the surrounding tephra
 342 ring.

343 The volcanoclastic diatreme infill has been categorised
 344 into eight lithofacies that have been grouped into five litho-
 345 facies associations (LFA) (Fig. 4 and Tables 1–2). These
 346 distinctions are based on differences in composition and
 347 textural characteristics. The diatremes appear to have a

Fig. 4 **A** Photograph of a pelletal lapillus with multiple coatings of basalt within structureless mLT (Borehole 28, 139.6 m). **B** Large Waulsortian Limestone clasts with alignment of smaller clasts around embayed edges in mLT (Borehole 28, 514.5 m). **C** ‘Raggy’ juvenile lapillus with flattened, irregular shape (Borehole 19, 54.9 m). **D** Well-sorted fines-rich pipe intruding into lapillistone within the bLT, outlined in dashed red lines (Borehole 28, 26.7 m). **E** Equal-sized globular juvenile lapilli with no interstitial ash matrix and slight welding within mLT (Borehole 19, 553.0 m). **F** Lithic-rich poorly sorted massive lapilli tuff with Waulsortian Limestone and dyke clasts as well as blocky juvenile lapilli (examples outlined in dashed red lines). Pervasive red discolouration is attributed to dolomitisation of mLT (Borehole 19, 491.7 m). **G** SEM image of a deep crustal xenolith comprising titanium oxide and magnetite coated with vesicular basalt (Borehole 19, 274 m). **H** Vesicular lapillus in the upper diatreme containing feldspar micro-phenocrysts and vesicles filled with chlorite (Borehole 19, 50 m). *Ab*, Albite; *Ca*, Calcite; *Ch*, Chamosite; *Mt*, Magnetite; *Sa*, Sanidine; *TiO*, Rutile

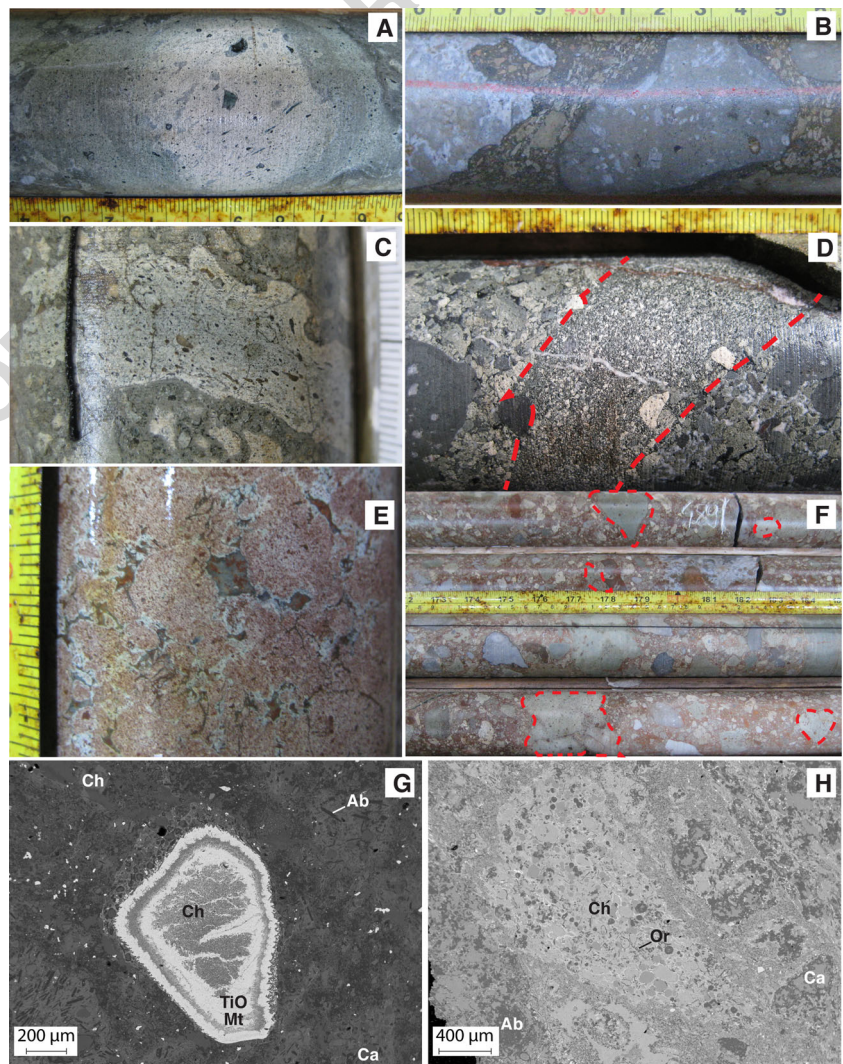


Table 1 Summary of lithofacies characteristics, context and interpretation for each lithofacies association in the diatremes

LFA	Litho	Description	Interpretation
1	Massive lapilli tuffs (mLT)	Predominantly massive, well-sorted lithofacies with high proportion of juvenile fine ash matrix altered to chlorite and locally infilled by carbonates.	Mass wasting of maar-diatreme walls and deposition by gravity flows in an open crater; possible elutriation of ash from lower in the system.
1	Lapillistones (Lf)	Structureless and clast supported with small lapilli and a low proportion of matrix; juvenile bombs and large lithic clasts present. Localised 'raggy' juvenile lapilli, preferred vertical orientation of clasts and apparent welding.	Fluidisation of hot lapilli in the central diatreme and transportation of outsized lithic clasts from lower in the stratigraphy
2	Bedded lapilli tuffs (bLT)	Highly heterogeneous lithofacies consisting of both massive and normally graded beds containing a high proportion of juvenile lapilli and highly variable proportion of fine ash matrix. Locally pockets of fine ash, pyrite and secondary calcite occur.	Subsided maar strata deposited near-vent as dilute density currents and later undercut by diatreme widening, leading to downward slumping along margins.
3	Massive lithic-rich lapilli tuffs (mlLT)	Structureless lithofacies locally with abundant lithic clasts and blocks, pervasive red-brown discolouration and fines-rich pockets and pipes.	Homogenous and structureless nature and degassing structures indicate fluidisation of diatreme fill.
3	Lithic-rich graded lapilli tuffs (l(n)LT)	Very poorly sorted, containing a high proportion of ash matrix and abundant juvenile lapilli and lithic blocks. Graded bedding with clast alignment, fines pockets and localised red-brown discolouration.	Accumulation through collapses of the country rock walls and overlying maar.
4	Lapilli tuffs (LTf)	Well-sorted highly altered lithofacies with a large proportion of matrix and lithic clasts. Localised small-scale grading, alignment of clasts, orange-red discolouration and localised injection of the tuffs into cracks in the country rock.	Deposited by a high pressure fluidised flow capable of dilating cracks in country rock.

348 central massive section with localised country rock breccias toward the base. The upper parts of the diatremes and margins consist of bedded lapilli tuff. Intrusions of variable thickness occur within the diatremes and to a lesser extent in the adjacent country rock. Juvenile lapilli lack macroscopic phenocrysts and are characterised by a low proportion of vesicles (typically 2–25 %). The majority of volcanoclastic material has been altered to clay, overprinting most primary textures and micro-phenocrysts. Ore forming minerals such as sphalerite and galena occur within the base of the diatremes in small quantities, visible under the SEM. This study focused on diatremes 19 and 28 as these preserve the most complete records and are covered by magnetic surveys and drill cores intersecting the central and marginal facies down to 560 m. In contrast, diatremes 47 and 77 were only sampled intermittently, as the drill core alternates between limestone and volcanoclastic material which has been brecciated and remobilised by later hydrothermal fluids forming polymict BMBs.

Table 2 Summary of measured characteristics of juvenile lapilli and lithic clasts, and vesicle size and percentage for each lithofacies association in the diatremes

LFA	Lithofacies	Juv. %	Juv. size (mm)	Lithic %	Lithic size (mm)	Matrix %	Ves. %	Ves. Av %	Ves. size (µm)
1	mLT	95–100	2–11	0–3	3–7	50–60	8–23	15	30–3000
1	Lf	98–100	2–48	0–2	5–16	15–25	12–24	19	12–2000
2	bLT	80–99	2–18	1–4	10–39	15–60	2–33	13	119–23,500
3	mlLT	65–90	2–52	10–17	3–71	15–70	4–58	17	6–11,300
3	l(n)LT	65–95	2–76	4–35	5–1670	20–30	4–8	15	134–3200
4	LTf	71–87	2–8	11–29	5–25	60–70	–	5–25	–

368 **Lithofacies characteristics**

369 *LFA 1: massive lapilli tuffs (mLT) and lapillistones (Lf)*

370 This lithofacies association is exemplified within the upper
 371 130 m of the centre of diatreme 19, consisting of two
 372 key lithofacies, massive lapilli tuffs and lapillistones that
 373 grade into each other with no visible bedding. The mas-
 374 sive lapilli tuffs (mLT) consist of well sorted fine to coarse
 375 ash, lack structure and grade downwards into a more lapilli-
 376 rich tuff. The proportion of juvenile material is high at
 377 approximately 95–100 % with only 0–3 vol. % country rock
 378 limestone fragments (see Table 2) and < 5 % pelletal lapilli
 379 (see Fig. 4a). These predominantly subspherical pelletal
 380 lapilli consist of as many as three rims of incipiently vesic-
 381 ular juvenile material surrounding lapilli of volcanoclas-
 382 tic material, carbonate country rock, or highly crystalline
 383 metamorphic lithic fragments. The rocks contain 40–72 %
 384 lapilli and 1–4 % blocks, with matrix proportion varying
 385 between 30 and 70 % but averaging around 60 vol. %,
 386 consisting mainly of fine ash. Clasts are sub-angular to
 387 sub-rounded and vary between 2–11 mm. Juvenile lapilli
 388 tend to be blocky and incipiently to poorly vesicular (8–
 389 23 %, Table 2). The lithofacies has a pervasive green
 390 colouration due to extensive alteration of ash and lapilli to
 391 chlorite. Localised areas (decimetre to metre scales) have
 392 experienced Fe stained carbonate replacement of the ash
 393 matrix.

394 The lapillistones (Lf) are similar in composition and
 395 structure to the more lapilli-rich mLT but contain 75–81 %
 396 lapilli, < 1–4 % blocks and only 15–25 vol. % matrix,
 397 which predominantly consists of fine ash altered to chlo-
 398 rite. Although the average juvenile lapillus is ~4 mm, the
 399 occasional limestone block reaches 48 mm. The juvenile
 400 lapilli have a measured vesicularity of 12–24 % (Table 2)
 401 similar to the mLT, and a low proportion of feldspar micro-
 402 phenocrysts (see Fig. 4H). Within the lithofacies, larger
 403 ‘raggy’ juvenile lapilli (see Ross and White (2012)) occur
 404 in addition to a localised sub-vertical clast orientation and
 405 partial welding.

406 *Interpretation of LFA 1*

407 The lapilli tuffs and lapillistones may have accumulated
 408 through a combination of progressive mass-wasting of the
 409 maar-crater walls (Gernon et al. 2009a) and preferential
 410 transport of fine ash to the upper part of the diatreme via
 411 gas-particle dispersions (Gernon et al. 2009b). Winnowing
 412 of fine ash from areas of LFA1 formed a large proportion
 413 of secondary pore space and high permeability allowing
 414 precipitation of a carbonate infill surrounding the lapilli
 415 (Davies et al. 2008). The blocky nature and incipient vesic-
 416 ularity suggest the lapilli were formed by fragmentation as

a result of magma-water interaction (Houghton and Wilson 417
 1989; Mattsson 2010). 418

The pelletal lapilli most likely formed when a dyke or sill 419
 intruded earlier water saturated volcanoclastic infill. Intense 420
 magma degassing combined with vaporisation of the dia- 421
 treme fill produced powerful gas jets in which globules of 422
 melt-coated clasts scavenged from the adjacent deposits (cf. 423
 Gernon et al. (2012)). Another theory suggests agglutination 424
 of small melt droplets to a core in the deep magma plumbing 425
 system (Lloyd and Stoppa 2003). These lapilli were likely 426
 transported from depth to the top of the diatreme by debris 427
 jets (Ross et al. 2008a; Valentine 2012) as evidenced by the 428
 vertical orientation of clasts (cf. White (1991)) and partial 429
 welding. 430

LFA 2: Bedded lapilli tuffs (bLT) 431

Bedded lapilli tuffs occur near the margins in the upper 432
 ~80 m of diatreme 28. Bed thickness varies considerably, 433
 averaging between 2 and 8 cm, but reaching up to several 434
 metres thick and generally increasing with depth. Transi- 435
 tions between beds are either sharp or diffuse, with normal 436
 and inverse grading observed, typically towards the base of 437
 beds. Bedding angles vary between 4 and 52°. On aver- 438
 age, beds contain 50–60 % ash matrix, pervasively altered 439
 to chlorite with pockets of secondary calcite and pyrite, 440
 decreasing to <15 % in clast supported beds. Lapilli propor- 441
 tions vary from 40 to extremes of 85 % and blocks <1 %. 442
 The degree of sorting decreases with depth, with upper- 443
 most beds well sorted and the lowest moderately sorted. 444
 Clasts are predominantly rounded and consist of 80–95 % 445
 juvenile material, 1–4 % limestone clasts and 3–20 % dark 446
 and blocky lapilli of low average vesicularity and possi- 447
 ble juvenile origin. Clast sizes vary from 2 to 40 mm but 448
 most juvenile particles are small, averaging between 2 and 449
 4 mm. Juvenile lapilli are non to incipiently vesicular (2– 450
 25 % vesicles), typically altered to chlorite and many have 451
 a dark green outer rim. 452

Interpretation of LFA 2 453

The sequence of thin beds is characteristic of frequent, 454
 small-scale phreatomagmatic eruptions (Lorenz 1986; Sohn 455
 1996; McClintock and White 2006). The nature of bedding, 456
 high degree of sorting, grading and rounded nature of clasts 457
 within this lithofacies suggests they were deposited in the 458
 maar crater from a series of dilute density currents (Cas 459
 and Wright 1991; White 2000). Very thin beds of tuff may 460
 be attributed to fallout of ash from suspension in the water 461
 column (White 2000). The rounded nature of the clasts sug- 462
 gests mechanical alteration of their shape by collisions and 463
 abrasion during transport in currents and debris jets (Cal- 464
 vari and Tanner 2011) or by recycling of juvenile material 465

466 by later eruptions (Houghton and Smith 1993; Leahy 1997).
 467 Alternatively, mass wasting of the maar-diatreme walls and
 468 introduction of water-supported gravity currents could have
 469 introduced this material into the open crater (cf. Gernon
 470 et al. (2009a)). The dark green rims to juvenile lapilli are
 471 interpreted as altered glass, thought to represent quenched
 472 margins that formed during ejection of hot pyroclasts into
 473 the water column. These quenched margins suggest that the
 474 lapilli were ejected molten and therefore capable of plasti-
 475 cally deforming during the expansion stage of magma-water
 476 interaction, providing another possible explanation for their
 477 round shapes (Kokelaar 1986). Progressive deepening of the
 478 diatreme would have caused widening and undercutting of
 479 the maar and slumping along the diatreme margins (Lorenz
 480 and Kurszlauskis 2007). These wedges of pyroclastic mate-
 481 rial and their associated bedforms (Fig. 1) are commonly
 482 preserved along the margins of diatremes and may result
 483 from fluidisation of a central region, which effectively
 484 destabilises the marginal deposits causing them to slump
 485 downwards (Gernon et al. 2008). The dark non-vesicular
 486 lapilli that comprise up to 20 % of this lithofacies are simi-
 487 lar to ‘blocky’ clasts described by Fisher (1984), Houghton
 488 et al. (1999) and Ross and White (2012). These are inter-
 489 preted as cognate clasts of either fragmented dykes intruded
 490 into the diatreme-fill (cf. Gernon et al. (2013)) or poorly
 491 vesicular magma that experienced brittle fragmentation (cf.
 492 Ross and White (2012)).

493 *LFA 3: Massive lithic-rich lapilli tuffs (mLT) and*
 494 *lithic-rich graded lapilli tuff (l(n)LT)*

495 The central part of the diatremes (e.g. diatreme 19) con-
 496 sists largely of massive lithic-rich lapilli tuffs with localised
 497 lithic-rich graded lapilli tuffs, penetrated by many late-
 498 stage vesicle and phenocryst poor intrusions, commonly
 499 exhibiting undulating contacts. Intrusions vary in thick-
 500 ness from tens of centimetres to 45 m, averaging at 2.5 m
 501 thick. However, intrusion angles vary between 2 and 69°
 502 from the horizontal, averaging 37°. Changes within the
 503 mLT lithofacies are gradual with no visible beds and
 504 an increasing proportion of matrix with depth from 15
 505 to 70 % and 30 to 85 % lapilli and no blocks between
 506 ~110–330 mbgs with localised variations. The lower part
 507 of diatreme 19 (c. 390–560 mbgs) contains a high pro-
 508 portion of clasts and only ~35 % matrix consisting of
 509 varying proportions of medium grained ash, limestone lithic
 510 clasts and localised patches of pyrite disseminated within
 511 the matrix. Clasts have angular shapes towards the top
 512 of the lithofacies but become rounded with depth, with
 513 26–73 % lapilli and 3–7 % blocks at the diatreme base.
 514 Juvenile lapilli remain dominant (65–90 %), with higher
 515 proportions of limestone country rock clasts (up to 17 %) and
 516 < 1 % lower crustal xenoliths coated with juvenile

material (Fig. 4G). Limestone clasts frequently exhibit
 embayed edges and a thin dark rim, possibly consisting of
 a mud coating (Houghton et al. 1999; Brown et al. 2008a).
 The average juvenile lapilli size is larger (6–13 mm) than
 within the upper diatreme, with local variations in sorting
 and maximum clast size reaching 76 mm. The proportion
 of dark incipiently vesicular material varies considerably
 between <5 and 90 % of the clast population and includes
 small lapilli to large blocks. The upper lithofacies is lack-
 ing in fine ash while the lower section contains isolated
 pockets and pipes rich in ash sized particles. Juvenile
 lapilli exhibit vesicularity ranging between 4 and 58 %
 and show a wide diversity in habit throughout the litho-
 facies. These include blocky with fracture-defined edges,
 areas of equigranular lapilli with little or no interstitial ash
 matrix and large ‘raggy’ lapilli. Pelletal lapilli commonly
 display multiple coatings of pale and dark magmatic mate-
 rial. Thin lapilli-rich and fines-rich pipes (1–4 cm wide) and
 partial welding are visible within the sequence. These parti-
 ally welded areas are usually found adjacent to boundaries
 such as dykes, veins or fractures and involve elongation
 parallel to the boundary and partial merging of juvenile
 particles.

An orange colouration, initially related to alteration of
 juvenile lapilli, starts at ~288 mbgs in borehole 19, locally
 at 182 mbgs in borehole 28 and intermittently at 295 mbgs
 in borehole 23. Towards the base of the diatremes, the altera-
 tion and discolouration of both clasts and matrix becomes
 more persistent and juvenile lapilli appear bleached (e.g.
 Fig. 4F). XRD analysis has shown that this alteration is the
 result of increasing dolomitisation with depth (Elliott et al.,
 unpublished data).

The l(n)LT units have sharp contacts with the surround-
 ing mLT and are characterised by a high concentration
 (up to 23 %) of blocks up to 1.7 m in diameter (79–
 100 % of which are country rock clasts) and 57–79 %
 lapilli. These units are poorly sorted with clast sizes aver-
 aging 11 mm, and a large range in angularity from sub-
 angular to well rounded. The units are lithic-rich with
 4–30 % limestone clasts and approximately 3 % dark
 LABL clasts and between 65 and 95 % juvenile lapilli,
 including up to 10 % dark, blocky incipiently vesicular
 clasts. Beds are typically graded with alignment of smaller
 clasts around larger clasts, and fines-rich pockets are also
 observed (Fig. 4D).

Interpretation of LFA 3

The massive nature of mLT is consistent with the
 homogenisation of a large part of the diatreme fill, partly
 through the action of debris jets (Lorenz 1975; Valentine
 2012; Delpit et al. 2014) and gas-fluidisation (Walters et al.
 2006; Gernon et al. 2008).

568 The majority of lapilli found within this lithofacies are
 569 blocky with fractured boundaries, and likely result from
 570 phreatomagmatic fragmentation (Fisher 1984; Houghton
 571 et al. 1999; Ross and White 2012). ‘Raggy’ clasts retain
 572 enough heat to remain in a hot plastic state (Ross and
 573 White 2012) as evidenced by their elongate shape and
 574 uneven edges, effectively moulding around adjacent clasts
 575 during transport (Fig. 4C). Globular lapilli are considered
 576 to result from gas streaming through magma, fragment-
 577 ing and depositing hot lapilli and welding grain boundaries
 578 (Fig. 4E). This process is similar to that described by Ger-
 579 non et al. (2012) for the formation of pelletal lapilli and
 580 is consistent with the high degree of sorting and paucity
 581 of fines.

582 The localised lithic-rich graded lapilli tuffs within the
 583 mLt are thought to be lenses of material resulting from
 584 episodic diatreme wall collapses or formed from explosions
 585 near the diatreme-country rock margin (Ross and White
 586 2006). The proportion of country rock is higher toward
 587 the base of the mLt (>250 mbgs), possibly because the
 588 limestone clasts are larger and denser and cannot easily be
 589 propelled by fluidising gases or debris jets (Valentine 2012).
 590 The undulating nature of intrusion margins indicates that
 591 they were emplaced prior to consolidation of the diatreme
 592 fill (Valentine 2012).

593 *LFA 4: Lapilli tuffs (Ltf)*

594 This lithofacies is closely associated with the brecciated
 595 country rock-diatreme contact, either as undulations in the
 596 diatreme walls or injected into fractures in the country
 597 rock. This lapilli tuff commonly grades downwards into a
 598 polymict black matrix hydrothermal breccia, not discussed
 599 in this paper. Defining characteristics include a high propor-
 600 tion of fine juvenile ash and limestone matrix (60–70 %),
 601 large clasts (Fig. 4B) and alignment of small juvenile lapilli
 602 around the country rock contacts. Proportions of clasts are
 603 variable with ~70–90 % juvenile lapilli and a high pro-
 604 portion of limestone (~10–30 %). Both juvenile and lithic
 605 clasts are sub-angular to well rounded and limestone clasts
 606 frequently show embayed edges (see Fig. 4B). Clast sizes
 607 range from 2 to 86 mm with a low degree of vesicularity (5–
 608 25 %). This unit is highly altered with red-brown dolomiti-
 609 sation increasing with depth and proximity to country wall
 610 contact.

611 *Interpretation of LFA 4*

612 Brecciation of the diatreme walls may be due to late-stage
 613 mass wasting (Gernon et al. 2009a), wall rock collapses dur-
 614 ing pipe excavation (Sparks et al. 2006), or alternatively
 615 by phreatomagmatic explosions when rising magma inter-
 616 acts with water-saturated diatreme fill (Lorenz et al. 2002;

Lorenz and Kurszlauskis 2007). These processes would cre- 617
 ate a highly permeable network of fractures, exploitable 618
 by fluidised lapilli tuff and magmatic intrusions. Smaller- 619
 scale features of ash and lapilli injected into cracks sug- 620
 gest that the lapilli tuff was fluidised and under sufficient 621
 pressure to further fragment the country rock. Irregular, 622
 embayed edges of larger limestone clasts suggest they have 623
 encountered acidic hydrothermal fluids after brecciation 624
 (Hitzman et al. 2002; Redmond 2010). The increased evi- 625
 dence for fluid interaction in this lithofacies suggests these 626
 fluids preferentially flowed along the limestone-diatreme 627
 contact. 628

Knockroe Formation 629

The Knockroe Formation within the Limerick study area 630
 is a 5 to 155-m-thick suite of alkali basaltic pyroclastic 631
 strata and lavas (Fig. 7). Several boreholes <1 km from 632
 the diatremes containing Knockroe pyroclastic rocks were 633
 sampled at a range of depths between 6 and 178 m and 634
 analysed for trace element concentrations by solution ICP- 635
 MS. Our data shows the Knockroe Formation to exhibit 636
 very similar trace and REE patterns to that of the dia- 637
 tremes (Fig. 5a). The Knockroe average lies consistently 638
 below that of the diatremes, which may represent dilution 639
 by the uptake of Mg and other elements during alteration 640
 in seawater (Humphris and Thompson 1978; Seyfried and 641
 Mottl 1982; Utmann et al. 2002). Zr is plotted against 642
 Nb (Fig. 5b) as Zr is considered relatively immobile under 643
 hydrothermal conditions (MacLean 1980; Rollinson 1993; 644
 Zhou et al. 2000), and Nb is highly incompatible and will 645
 therefore be enriched in early mantle melts. The Knockroe 646
 samples clearly follow the same linear pattern and Nb/Zr 647
 gradient as the diatreme samples, indicating that they fol- 648
 low a similar fractionation trend. These data show a clear 649
 genetic link between the diatreme and Knockroe Formation, 650
 suggesting the latter formed predominantly by diatreme 651
 sourced material. 652

Various parts of the sequence are interbedded with cherty 653
 wackestones of the Lough Gur Formation. The Knockroe 654
 Formation is divided into five different lithofacies based 655
 on their textural characteristics and depositional processes 656
 and numbered in depositional order (Fig. 6). The fine- 657
 grained lithofacies 1 occurs at the base of three of the 658
 boreholes but thins out toward the SE, exhibiting normal 659
 grading and commonly fine laminations in beds that vary 660
 from <0.1–1 m thick. Typically, these beds are overlain 661
 by dark lapilli-rich lapilli tuff (lithofacies 2). Lithofacies 2 662
 grades upwards into a fines-poor unit (lithofacies 3) with 663
 larger rounded lapilli with clay or ash matrix near the base 664
 and small lapilli with ash matrix near the top. The over- 665
 lying lithofacies 4 is typically interbedded with fines-poor 666
 material. Here, lapilli are sparse within the wackestones 667

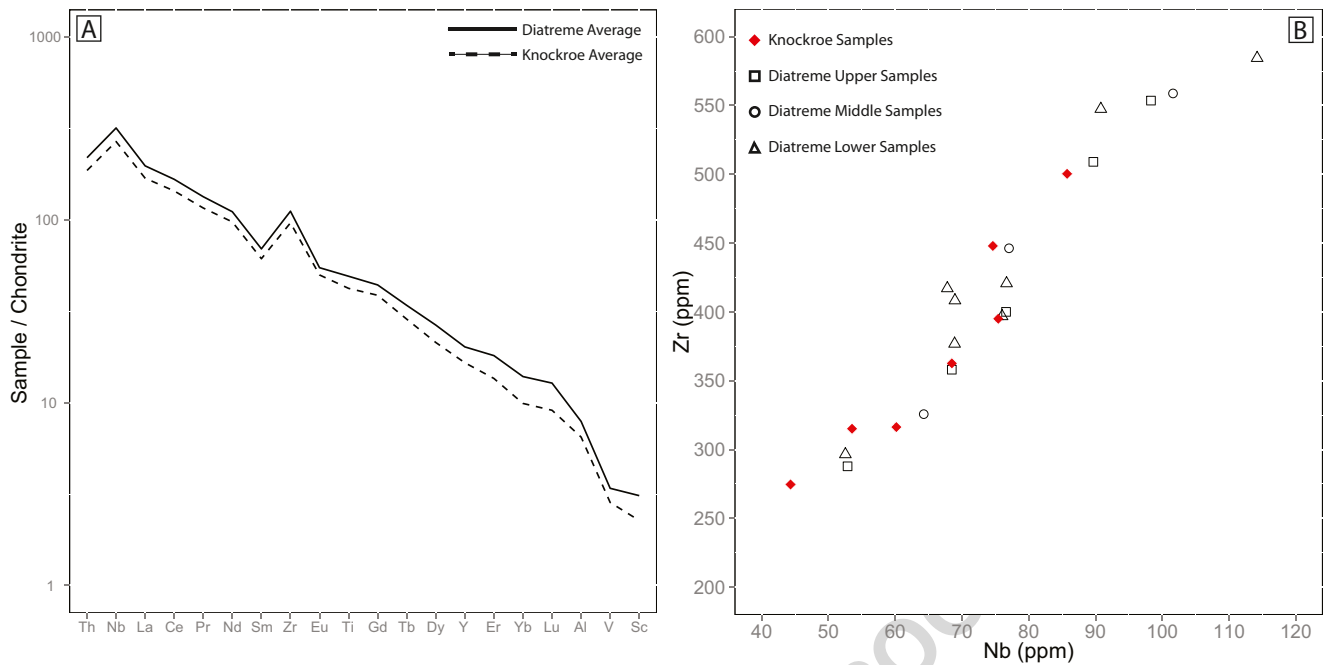


Fig. 5 Trace element data obtained by ICP-MS for diatremes (19 and 28) and the Knockroe Formation. **A** Multi-element plot shows two very similar trace element patterns for the two deposits. The Knockroe

average data are consistently slightly more diluted than that of the diatreme for all elements, most likely due to alteration in seawater, e.g., uptake of Mg. **B** Nb versus Zr plot showing very similar trends and trace element data for diatremes and the Knockroe Formation

668 or are interbedded with crinoidal debris in more con- 693
 669 centrated, thin beds and contain occasional volcanoclastic 694
 670 autoliths. At the top is lithofacies 5, a matrix-supported and 695
 671 poorly sorted massive unit, which predominantly contains 696
 672 altered volcanoclastic material and limestone clasts, textu- 697
 673 rally and compositionally resembling deposits of the upper 698
 674 diatreme. This lithofacies increases in thickness toward 699
 675 the SE from 1 m in borehole 24 to 25 m in borehole 700
 676 6 (Fig. 7) with beds typically dipping between 3–50°, 701
 677 averaging ~30°. 702

678 *Interpretation of the Knockroe Formation*

679 To the SW, the thickened Knockroe Formation truncates 706
 680 the carbonate formations, infilling a pre-existing topog- 707
 681 raphy most likely formed by carbonate mounds of the 708
 682 Waulsortian Limestone. Greywacke beds within the Knock- 709
 683 roe Formation were deposited during the Lower Viséan 710
 684 (345–399 Ma) (Somerville et al. 1992) in a shallow water 711
 685 submarine environment (Lees and Miller 1985; Holland and 712
 686 Sanders 2009). Deposition of these greywackes at Limerick 713
 687 is estimated to have occurred at water depths between 20 714
 688 and 120 m. This upper limit is based on the depth ranges 715
 689 proposed by Wood (1957), Riding (1975) and Gallagher 716
 690 and Somerville (2003) for foram and algae (taxa *Draffania* 717
 691 and *Girvanella*) observed in the Lough Gur beds by 718
 692 Somerville et al. (1992). The lower depth limit is based on 719

the lack of ooids in the Limerick upper Waulsortian that 693
 have been observed in other areas where this Formation 694
 has reached depths <120 m (Lees and Miller 1985), and 695
 also reflects the underlying carbonate bathymetry seen in 696
 Fig. 7. The thin to medium cross-laminated tuff beds of 697
 lithofacies 1 were most likely deposited from dilute turbid- 698
 ity currents linked to density flows. The thin discrete beds 699
 likely formed by ash fall from suspension in the water col- 700
 umn after Surtseyan-type pulses of activity (White 2000). 701
 The lithic content is negligible at <1 % indicating that 702
 any magma-water interaction was not diatreme-forming, 703
 due to the lack of country rock fragmentation. Any explo- 704
 sive magma-water interaction therefore most likely occurred 705
 at the water-sediment interface, rather than being confined 706
 within solid rock (Kokelaar 1986). Magma fragmentation 707
 within the submarine environment would also most likely 708
 involve cooling-contraction granulation processes (Koke- 709
 laar 1986), explaining the fine-grained lapilli and ash within 710
 this lithofacies. 711

Lithofacies 2 contains a high proportion of dark, blocky, 712
 non- to incipiently vesicular clasts that appear fresh com- 713
 pared to the surrounding juvenile material and contain small 714
 proportions of microcrystalline feldspar. These could repre- 715
 sent country rock lava fragments (Kurszlauskis et al. 1998; 716
 Gernon et al. 2013), disrupted sills (Nemeth et al. 2001) 717
 or fragmentation of a rapidly cooled melt (Ross and White 718
 2012). The appearance of limestone clasts possibly indicates 719

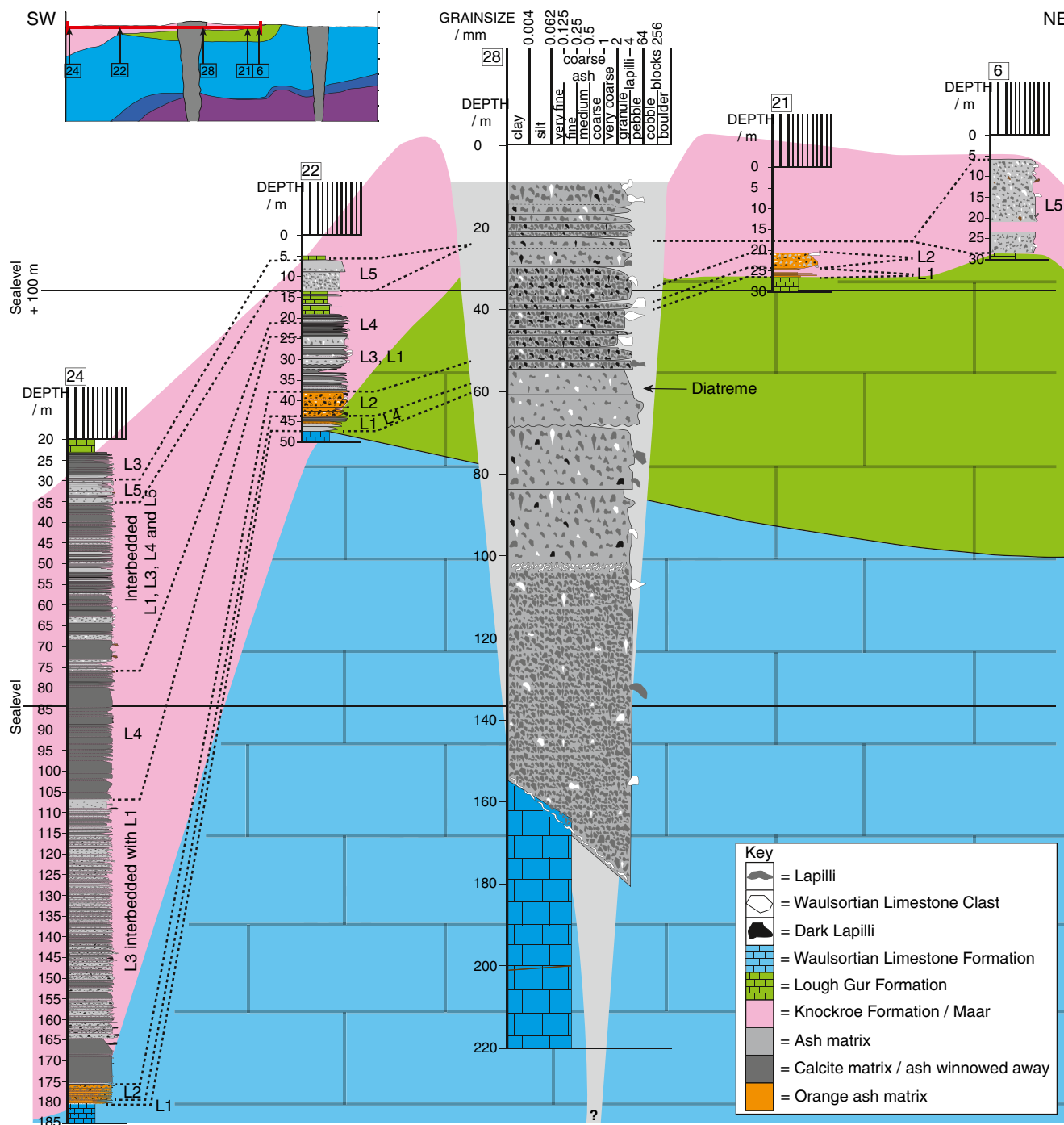


Fig. 6 Photographs of the Knockroe volcaniclastic formation divided into five lithofacies. *Arrows* indicate sample orientation, pointing toward the top of the borehole. **L5** Upper Knockroe, surrounding the diatreme, consisting of poorly sorted lapilli tuff with an altered *green ash matrix*. Lapilli are subrounded and incipiently vesicular, containing aligned feldspar phenocrysts. Clasts consist primarily of juvenile lapilli, dark blocky lapilli and Waulsortian Limestone. Beds tend to be very thick varying between 0.5 and 25 m. **L4** Greywacke beds with thin layers of volcaniclastic material. Beds vary greatly in thickness between 0.1 and 7 m and are matrix supported, containing 0–50 % lapilli and crinoidal debris. Lapilli are altered, incipiently vesicular and sub-rounded to rounded. Some beds contain rounded autoliths. **L3** Clast supported and normally graded beds usually 0.5–2 m thick,

predominantly juvenile lapilli with occasional limestone or crinoidal clasts. Clasts are sub- to well-rounded and range from pebble sizes at the base to sand grades of ash at the top. Spaces between the lapilli are filled with dark clays or calcite. Lithofacies may grade vertically into sections with an ash matrix. **L2** Typically occurs above the laminated tuff: packages of lapilli tuff between 5 and 10 m thick containing high proportions of blocky non to incipiently vesicular dark clasts. Other clasts include rounded chloritised juvenile lapilli and Waulsortian limestone; occasionally, altered orange and containing diatreme autoliths. **L1** Thin to medium beds (0.1–1 m thick) of often laminated and normally graded ash interbedded with lithofacies 2. Ash is moderately to poorly sorted and consists of non-vesicular juvenile material and blocky dark fragments

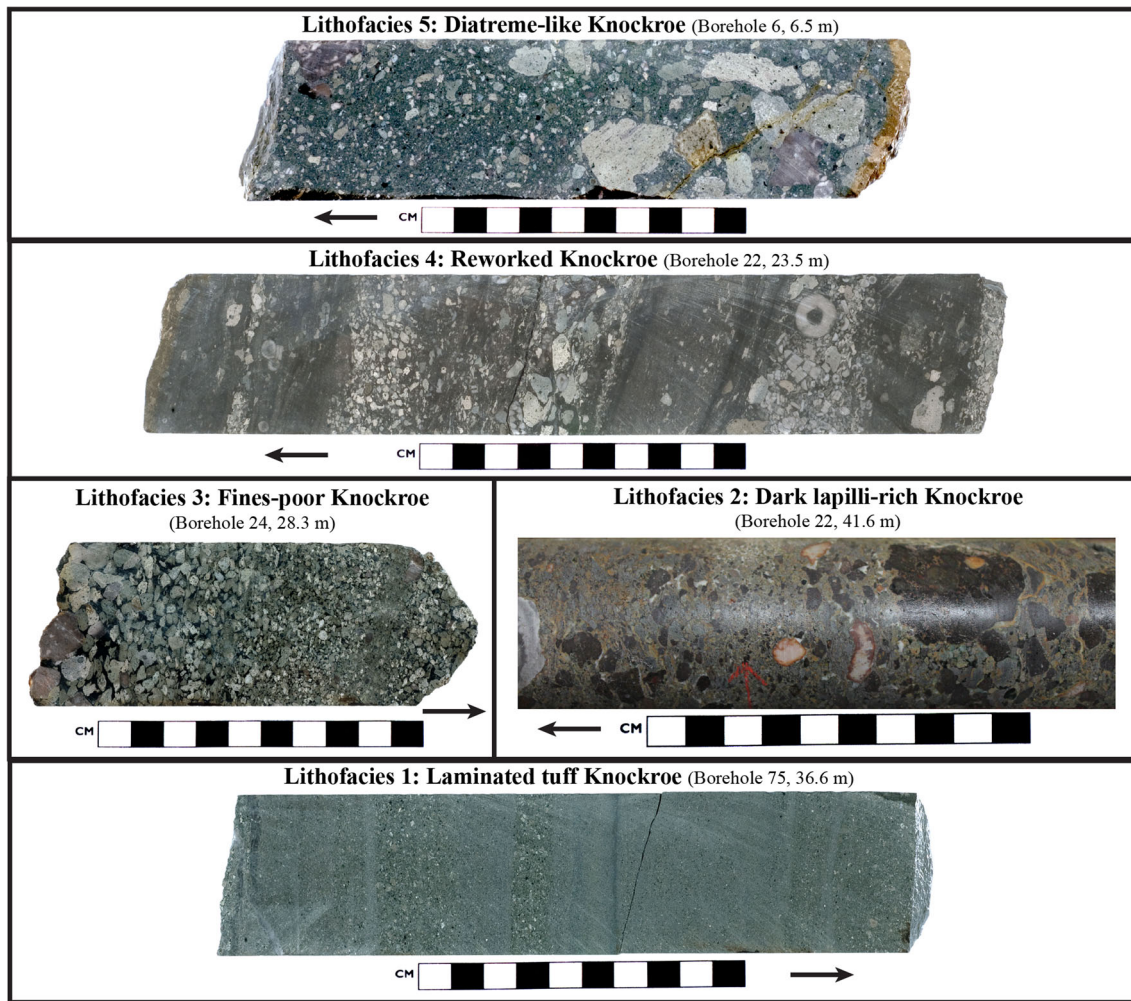


Fig. 7 Cross section from SW to NE, showing 4 logs of drillcore of the Knockroe Formation and their spatial relationship to a diatreme (shown in centre). The lateral extent of the diagram is indicated by the red line on the cross section (inset). Numbers in boxes at the top of the

logs indicate the borehole number. Dotted lines indicate where packages of beds have been correlated between the logs. Ln indicates the lithofacies package and relates to the lithofacies described in Figure 5

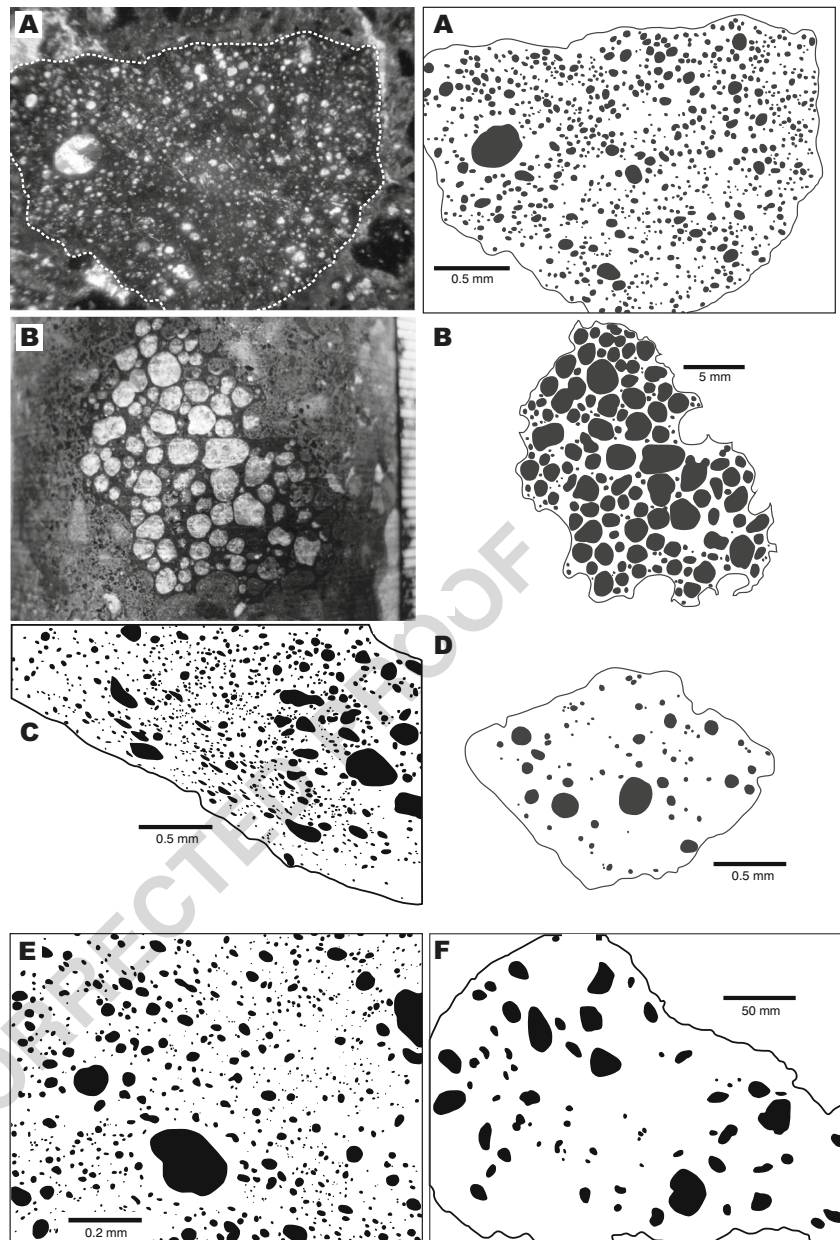
720 the onset of country rock fragmentation and diatreme-
721 forming phreatomagmatic activity (Lorenz et al. 2002; Ross
722 and White 2006).

723 The normally graded beds of lithofacies 3 most likely
724 formed in debris currents related to eruption column col-
725 lapse in water, that may or may not have breached the
726 water surface (Fiske et al. 1998). In this submarine envi-
727 ronment, these density currents would have been water-
728 supported (White 2000). These currents can be eruption-fed,
729 formed by rising tephra jets expanding and ingesting water
730 (White 2000), subsiding and flowing outward from the
731 volcanic centre. Alternatively, where the eruption col-
732 umn breaches the water surface, tephra and particles can
733 be deposited subaerially. High concentrations of particles
734 in the water column can lead to gravitational instabili-
735 ties and, forming vertical density currents (Fiske et al.

1998) that would be hard to distinguish from other
736 deposits. These water-supported currents deposit Bouma-
737 type sequences with concentrated basal flows depositing
738 massive unsorted units, grading up into stratified ash
739 beds deposited by the more dilute particle current above
740 (Mueller and White 1992; White 2000). The bases of such
741 sequences are not observed at Limerick, due to direct injec-
742 tion of tephra jets into the water column. This created
743 multiple pulses of more dilute eruption-fed flows deposit-
744 ing a series of unwelded and graded beds (Kneller and
745 Branney 1995; White 2000), similar to the typical upper
746 sequence.
747

Isolated beds of lithofacies 4, interbedded with fos-
748 siliferous debris, indicate a submarine eruption environ-
749 ment. The lithofacies is attributed to re-working of pre-
750 existing pyroclastic deposits, which were saturated, highly
751

Fig. 8 Examples of typical lapilli and digitised vesicles used in image analysis (vesicularity values shown in *brackets*). **A** Lower diatrema lapillus (11 %) in an ash and disseminated limestone matrix (Borehole 19, 274 m). **B** Upper diatrema lapillus (64 %) infilled with calcite (Borehole 28, 33.7 m). **C** Middle diatrema lapillus (21 %) with calcite infilling elongated vesicles (Borehole 19, 102 m). **D** Lower diatrema lapillus (21 %) with a high number density of small vesicles (Borehole 19, 274 m). **E** Knockroe lapillus (17 %) (Borehole 24, 86.7 m). **F** Knockroe lapillus (12 %) (Borehole 24, 28.2 m)

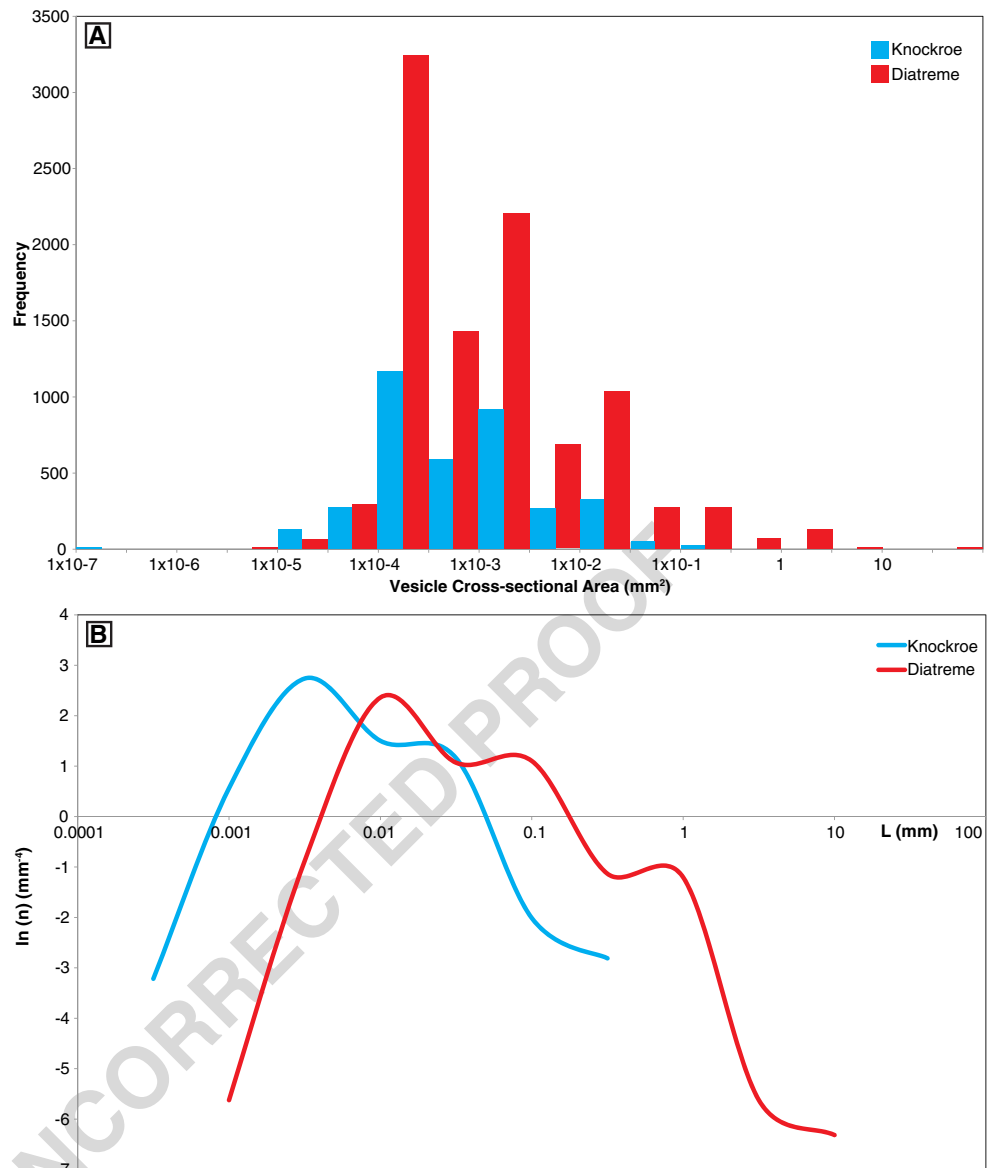


752 mobile and liable to slump (Fiske et al. 1998; White
 753 2000; Pittari et al. 2008). The Knockroe lithofacies are
 754 broadly comparable to the deposits of Bridge Point, New
 755 Zealand, where pauses in the Surtseyan-type eruption
 756 sequence are recorded by gradual resumption of normal
 757 sedimentation and re-working of abraded clasts and fossils
 758 (White 2000).

759 Beds of lithofacies 5 typically show normal grading
 760 at the top and inverse to non-graded bases, indicative of
 761 deposits of subaqueous debris flows (Nemec and Steel
 762 1984) similar to those observed at the Costa Giardini
 763 diatrema, southern Italy (Calvari and Tanner 2011). The

764 presence of Waulsortian Limestone clasts indicates breccia-
 765 tion of country rock at least 80 m below the seabed.
 766 This can occur during phreatomagmatic explosions (Lorenz
 767 et al. 2002; Lorenz and Kurszlaukis 2007), and/or dia-
 768 trema expansion by implosion, spalling or undercutting
 769 (Sparks et al. 2006). Juvenile lapilli reveal incipiently
 770 vesicular blocky shards (Fig. 6) suggesting magma frag-
 771 mentation by explosion rather than intense vesiculation
 772 (Heiken 1972; Houghton and Wilson 1989; Ross and White
 773 2012). All these features suggest the uppermost lithofa-
 774 cies resulted from high-density debris currents sourced from
 775 the diatremes.

Fig. 9 **A** Histogram of vesicle cross-sectional area versus frequency for juvenile lapilli from both the Knockroe Formation and diatreme deposits. Three modal categories are observed for the diatreme samples and two for the Knockroe samples, indicating separate nucleation events. **B** Plot of equivalent length against the natural log of the vesicle number density. The same nucleation events can be seen as modal values of the equivalent length and upturning at the end of the lines are interpreted as due to vesicle coalescence



776 **Vesicle distributions**

777 In general, the vesicularity within both diatreme 19 and
 778 Knockroe juvenile clasts is low. Vesicularity within the
 779 Knockroe Formation ranges between 6 and 50 %, averaging
 780 ~17 %, and in the diatremes varies between 2–63 %,
 781 averaging ~30 % (Fig. 8). Although, vesicularity is slightly
 782 lower in the Limerick samples, values are comparable to
 783 the emergent Surtseyan-type phreatomagmatic eruptions at
 784 Capelas, Azores (18–58 vol. %) and the phreatomagmatic
 785 deposits of Miyakejima, Japan containing 20–70 vol. %
 786 (Shimano and Nakada 2006; Mattsson 2010). The higher
 787 Limerick values lie within the range required for explosive
 788 magmatic activity (50–80 %; Houghton and Wilson (1989))
 789 and tend to be found at the base of the Knockroe Forma-
 790 tion and in the lower parts of the diatremes (~350–520 m

(Fig. 10). The magma fragmenting to form these lapilli at
 the base of diatreme 19 was likely more mature, having
 undergone a higher degree of coalescence.

Image analysis has captured a total of $\sim 0.0135 \times 10^6$
 vesicles (Fig. 9a). Figure 9b plots L , the equivalent vesicle
 length, against the natural log of n , the vesicle number
 density for vesicle lengths placed into the same categories
 used in Fig. 9a. The multiple modal values can be seen
 by the two changes in gradient for the Knockroe Forma-
 tion, and three for the diatreme, and indicate multiple
 nucleation events took place before magma fragmentation
 (Shea et al. 2010).

Clasts of the Knockroe Formation contain a population
 of smaller vesicles relative to diatreme 19 (Fig. 9) and
 exhibit two nucleation events, most likely material ejected at
 an early eruptive stage. Diatreme deposits record a third

807 population of larger vesicles which may reflect an addi- 807
 808 tional nucleation event or inflation of vesicles due to later 808
 809 outgassing as diatreme lapilli are insulated and capable 809
 810 of sustained plastic deformation. Both a positive and a 810
 811 negative gradient are shown (Fig. 9b), suggesting the vesi- 811
 812 cles were in the early stages of ripening (Shea et al. 812
 813 2010)—the process by which volatiles diffuse from high 813
 814 pressures present in smaller bubbles to regions of low 814
 815 pressure in larger bubbles (Mangan and Cashman 1996). 815
 816 Alternatively, these larger vesicles may have formed by 816
 817 maturing from nucleation to coalescence before eventual 817
 818 bubble wall relaxation. An upturning of the trend line 818
 819 (Fig. 9b) is interpreted as due to bubble coalescence (Shea 819
 820 et al. 2010). Figure 9a shows the majority of vesicles 820
 821 are smaller than $1.5 \times 10^{-2} \text{ mm}^2$ cross-sectional area. 821
 822 Tsukui and Suzuki (1995) suggested that vesicles smaller 822
 823 than $2 \times 10^{-1} \text{ mm}^2$ are the result of super-cooling-related 823
 824 nucleation resulting from quenching during phreatomag- 824
 825 matic eruptions (Mattsson 2010). However, (Shimano and 825
 826 Nakada 2006) suggest that smaller bubble fractions are 826
 827 unrelated to fragmentation method and solely represent 827
 828 the high rate of magma decompression and eruption 828
 829 (Mattsson 2010).

In general, vesicularity increases with depth within 830
 diatreme 19 (Fig. 10) indicating an increasing impor- 831
 tance of exsolving gas in the eruption processes. How- 832
 ever, the majority of lapilli within the central diatreme 833
 and Knockroe Formation exhibit incipient to poor vesicu- 834
 larity (averaging 14–21 %), well below that required for 835
 fragmentation by rapid bubble growth, suggesting frag- 836
 mentation by an external water source. The Knockroe 837
 Formation only record two nucleation events, whereas dia- 838
 treme 19 record three events (Fig. 9); this is attributed 839
 to more rapid quenching of ejecta in the water col- 840
 umn, relative to thermally insulated pyroclasts in the dia- 841
 treme, which are capable of more sustained degassing and 842
 vesiculation. 843

Discussion 844

On the basis of the observed structural, compositional 845
 and textural characteristics of these lithofacies associations 846
 (Table 1), we propose a multi-stage phreatomagmatic and 847
 magmatic model for the eruption of diatremes within the 848
 Limerick cluster (Fig. 10). 849

Initial eruption stage 850

The thin, well-sorted and graded beds deposited near the 851
 base of the Knockroe Formation by dilute density currents 852
 (see Fig. 8) show similarities with well-documented sub- 853
 aqueous and submarine eruptions such as those of Iblean, 854
 Southern Italy (Calvari and Tanner 2011) and Pahvant 855
 Butte, Utah (White 1996), resulting from Surtseyan-type 856
 eruptions (White 2000; White and Houghton 2006; Cal- 857
 vari and Tanner 2011). The paucity of lithic clasts in 858
 lithofacies 1 indicates initial eruptions did not involve sig- 859
 nificant country rock brecciation and were not diatreme 860
 forming. 861

Diatreme juvenile lapilli contain very low concentrations 862
 of feldspar micro-phenocrysts (Fig. 4h). This paucity of 863
 phenocrysts might suggest that the parent magmas experi- 864
 enced rapid volatile driven ascent from lower crustal 865
 levels, as evidenced by the presence of deep crustal xeno- 866
 liths in the diatreme fill (Fig. 4g) and in the Knock- 867
 roe Formation (Redmond 2010). Rapid magma ascent 868
 rates would prevent both extensive crystallisation and 869
 interaction with water (Valentine 2012), preventing coun- 870
 try rock brecciation (cf. Gernon et al. (2013)) (Fig. 871
 11). Explosive magma-water interaction at the sediment- 872
 water interface as well as cooling-contraction granula- 873
 tion (Kokelaar 1986) fragmenting the hot clasts, most 874
 likely accounts for the fine-grained nature of the basal 875
 Knockroe lithofacies. 876

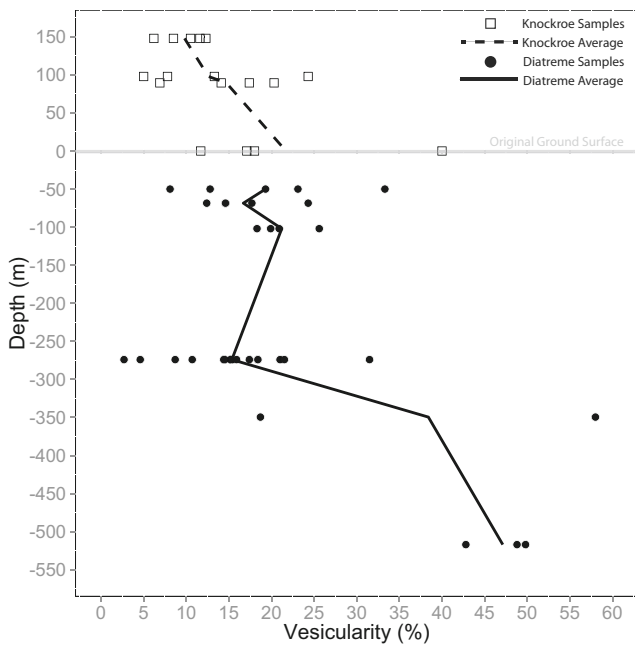
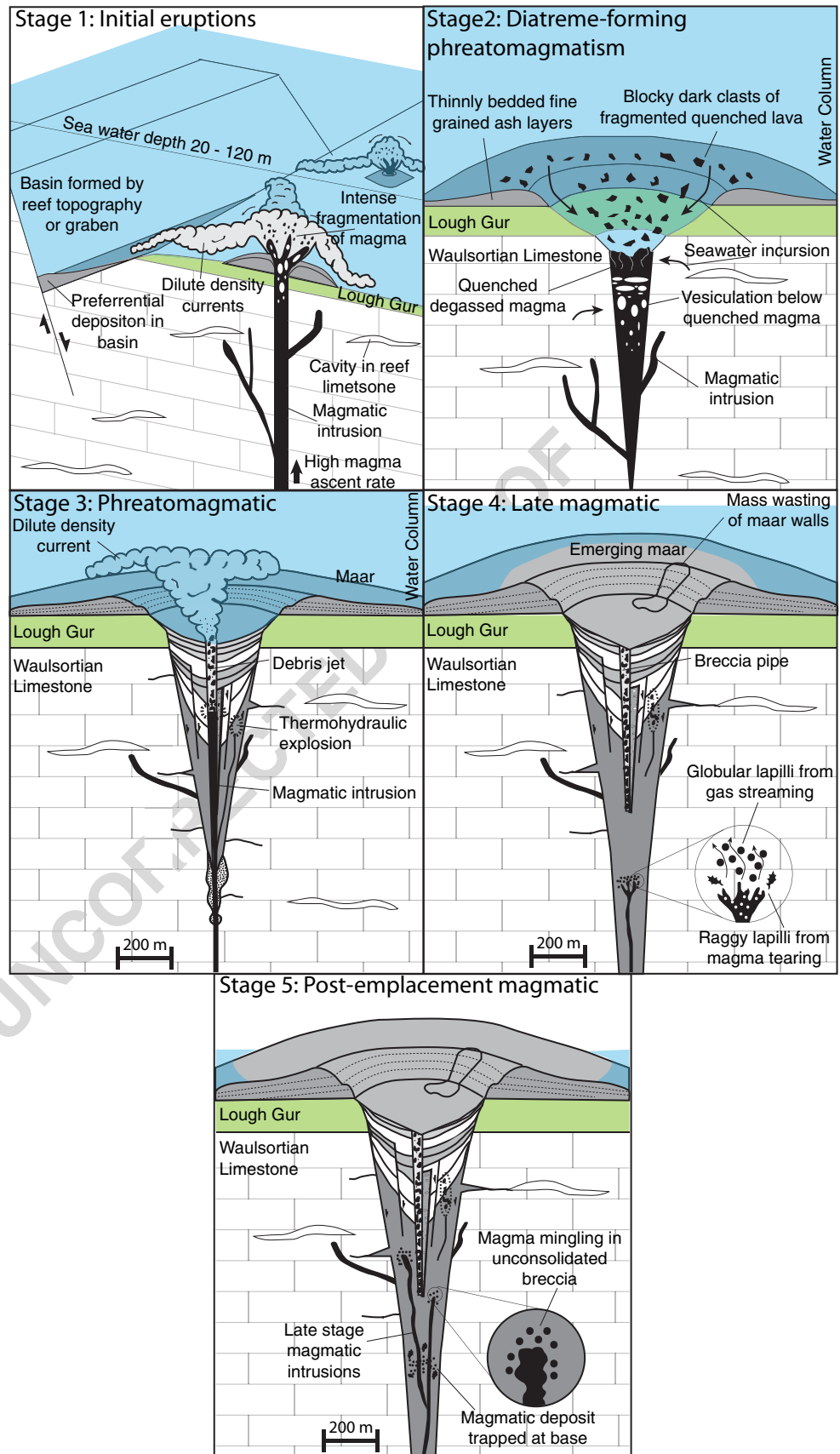


Fig. 10 Graph showing ranges and mean values of clast vesicularity in both Knockroe and diatreme deposits. Knockroe borehole 24 and diatreme borehole 19 have been used for this graph as they contain the most complete records of volcanoclastic material. Note that vesicularity generally increases with depth in both environments. The zero line represents the original ground surface upon which the Knockroe extra-crater material would have been deposited, creating positive topography. Diatreme sample depths are indicated by negative numbers

Fig. 11 Schematic cartoon illustrating the five stages of diatreme emplacement (see discussion). Stage 1 shows eruption sites shedding pyroclastic material via dilute density currents into the adjacent basin. Stage 2 depicts the onset of phreatomagmatic activity. Sea water incursion through the vent and fractured country rock forms a quenched non-vesicular body of magma which is fragmented and ejected by initial phreatomagmatic explosions. Stage 3 shows phreatomagmatic explosions producing debris jets that homogenised the central diatreme facies and widened the diatreme, undercutting overlying maar deposits. Stage 4 illustrates the late stage magmatic activity forming globular and 'raggy' lapilli, trapped at the base of the diatreme. Stage 5 involves post diatreme emplacement and non-explosive intrusion of magma into unconsolidated diatreme fill



877 **Transition to diatreme-forming phreatomagmatic**
878 **stage**

879 Within the Knockroe Formation, beds of lithofacies 2 con- 926
880 tain up to 40 % less-intensely altered vesicular dark lapilli 927
881 and up to 10 % limestone lithic clasts. The co-occurrence 928
882 of abundant juvenile clasts and country rock lithic clasts 929
883 are attributed to an onset of diatreme excavation by explo- 930
884 sive magma-water interaction. After an initially high magma 931
885 flux, water incursion into the vent within a submarine 932
886 environment would likely have led to rapid cooling and 933
887 fragmentation of magma, degassed during initial eruptions. 934
888 Further water incursion may have caused phreatomag- 935
889 matic explosions, brecciating the surrounding country rock 936
890 (Lorenz et al. 2002; Lorenz and Kurszlaukis 2007; Ross and 937
891 White 2006; Sparks et al. 2006) and ejecting both limestone 938
892 clasts and basalt in pulsatory explosions (Fig. 11). 939

893 **Phreatomagmatic stage**

894 Below the upper bLT, diatremes 19 and 28 consist 940
895 of massive lithic-rich lapilli tuffs (mLT) with localised 941
896 lithic-rich graded lapilli tuffs (l(n)LT). Homogenisation 942
897 of this deposit is considered to be the result of flu- 943
898 idisation by volatiles sourced from outgassing magma 944
899 (Sparks et al. 2006; Walters et al. 2006; Gernon et al. 945
900 2009b) or alternatively by conversion of water to steam 946
901 (White 1991; Lorenz and Kurszlaukis 2007), creating debris 947
902 jets. The blocky, fracture bound and incipiently vesicular 948
903 clasts, combined with high concentrations of lithic clasts 949
904 (10–35 %) suggest eruptions were caused by magma-water 950
905 interactions (Lorenz et al. 2002; Ross and White 2006). 951

906 After the initial high magma flux, seawater incursion into 952
907 the vent likely formed a mobile water-rich slurry into which 953
908 magma intruded (Kokelaar 1983). The rising magma would 954
909 have flash heated water within this slurry to steam, creat- 955
910 ing gas propelled jets of debris and localised fluidisation 956
911 of the diatreme fill (Kokelaar 1983; White 1991; Gernon 957
912 et al. 2009b). Upward transport of material by these two pro- 958
913 cesses and subsequent subsidence would have led to vertical 959
914 mixing and large scale homogenisation of the water-rich 960
915 mix (McClintock and White 2006; Gernon et al. 2009b; 961
916 Valentine 2012). Such processes and creation of debris jets 962
917 could explain the elutriated fines-rich pockets and pipes 963
918 observed at Limerick and many other diatreme sites (cf. 964
919 McClintock and White (2006), Ross and White (2006), 965
920 Brown et al. (2008a), Gernon et al. (2008), and Gernon et al. 966
921 (2013)). 967

922 Vesicularity studies support this interpretation, as vesi- 968
923 cle sizes and percentages are similar to Surtseyan-type 969
924 emergent phreatomagmatic eruption deposits at Capelas, 970
925 Azores and Miyakejima, Japan (Tsukui and Suzuki 1995;

Shimano and Nakada 2006; Mattsson 2010). This stage is 926
recorded by multiple pulses of debris flows (Nemec and 927
Steel 1984) recorded in lithofacies 3 of the Knockroe For- 928
mation, which contains large country rock lithic clasts and a 929
paucity of fines due to elutriation by turbulent flows. Similar 930
repetitive sequences are observed within maars in both sub- 931
aerial settings, e.g. the Joya Honda maar, Mexico (Aranda- 932
Gómez and Luhr 1996), and the Colli Albani maars, Italy 933
(Sottili et al. 2009), and in submarine settings, e.g. Iblean, 934
Southern Italy (Calvari and Tanner 2011). Pauses in pyro- 935
clast deposition are marked by the resumption of greywacke 936
sedimentation and may represent periods of inactivity or 937
alternatively phreatomagmatic activity that was too deep 938
for debris jets to breach the surface and eject material 939
(Ross and White 2006; Ross et al. 2008b; Valentine 2012; 940
Graettinger et al. 2014). Regional deposition of the Lough 941
Gur greywacke Formation occurred in water depths of 20– 942
120 m, indicating these diatremes initially erupted into 943
a significant body of water. The presence of greywacke 944
beds within the Knockroe Formation is thought to indicate 945
that basinal subsidence continued at rates comparable to 946
volcanic accumulation (Strogen 1988). 947

948 The large ‘raggy’ clasts were emplaced whilst still in 949
949 a hot plastic state (Ross and White 2012), after lim- 950
950 ited interaction with water. Although the majority of 951
951 juvenile clasts are incipiently vesicular, a small pro- 952
952 portion of larger clasts exhibits up to ~60 % vesi- 953
953 culation. Magma-water interaction can form a large 954
954 range in vesicularity depending on the degree of mag- 955
955 matic gas exsolution at the time of fragmentation 956
956 (Houghton and Wilson 1989). Although this prolonged 957
957 stage is dominated by phreatomagmatic activity, the greater 958
958 vesicularity of these lapilli indicates that magmatic pro- 959
959 cesses were still important. 960

960 **Late magmatic stage**

961 At the lowest observed levels in diatreme 19, the mLT con- 961
962 tains a higher ratio of juvenile to lithic clasts. Juvenile lapilli 962
963 have undergone a higher degree of vesiculation (~50–60 %) 963
964 and coalescence creating ‘frothy’ lapilli also observed in 964
964 the Joya Honda maar, Mexico (Aranda-Gómez and Luhr 965
965 1996). Here, this texture is attributed to low confining pres- 966
966 sure exerted on the magma during vent excavation, allowing 967
967 more advanced vesiculation before groundwater interaction 968
968 (Aranda-Gómez and Luhr 1996). Proportions of ‘raggy’ and 969
969 pelletal lapilli also increase, indicating a lower degree of 970
970 magma-water interaction toward the base of the diatreme. 971
971 These lapilli exhibit evidence for heat retention, including 972
972 fluid, plastically deformed shapes and partial sintering with 973
973 adjacent lapilli. A basaltic lava flow directly overlies vol- 974
974 caniclastic deposits of the Knockroe Formation less than 975

976 500 m to the south-west of diatreme borehole 28. The flow
 977 has not formed hyaloclastites or pillows and does not exhibit
 978 an extensive chilled margin, indicating eruption into a sub-
 979 aerial environment (Griffiths 1992; Gregg and Fink 1995;
 980 White 2000). This observation is consistent with the inferred
 981 decline in magma-water interaction and collectively are best
 982 explained by emergence of the system (Fig. 11) as sug-
 983 gested by Holland and Sanders (2009), explaining the lack
 984 of submarine fossiliferous debris in the upper Knockroe
 985 (lithofacies 5). Emergence and subsequent drying out of the
 986 diatreme may have caused a downward migration of explo-
 987 sion depths (Mattsson et al. 2005), prior to or during this
 988 late magmatic stage.

989 **Post-emplacement magmatic stage**

990 Late-stage intrusion of magma into unconsolidated
 991 diatreme-fill is a common feature of diatremes (Valen-
 992 tine 2012), as observed in the Gibeon Kimberlite
 993 Field, Namibia (Kurszlaukis et al. 1998), Iblean, Italy
 994 (Calvari and Tanner 2011) and Elie Ness, Scotland (Gernon
 995 et al. 2013). They represent late stage upwelling of magma
 996 soon after the cessation of explosive volcanic activity
 997 (Kurszlaukis and Barnett 2003; Lorenz and Kurszlaukis
 998 2007; Valentine 2012). Dense dark clasts are closely associ-
 999 ated with a ~1 m thick intrusion, and thought to result from
 1000 magma fragmentation upon contact with unconsolidated
 1001 diatreme fill, causing magma mingling and disintegration
 1002 into blocky clasts (White 2000; Calvari and Tanner 2011).

1003 **Conclusions**

1004 The Knockroe Formation records an initial eruption stage
 1005 of the Limerick diatremes, involving rapid magma ascent
 1006 from lower crustal levels. High ascent rates allowed
 1007 magma to reach the sediment-water interface before any
 1008 appreciable crystallisation or magma-water interaction
 1009 occurred, resulting initially in small (non-diatreme form-
 1010 ing) phreatomagmatic eruptions. An extended period of
 1011 phreatomagmatic activity formed diatremes of greater than
 1012 500 m depth filled with massive deposits homogenised
 1013 by fluidisation and debris jet action. Evidence for this
 1014 stage is recorded in the ~150-m-thick Knockroe Forma-
 1015 tion with interludes of sediment deposition (i.e. Lough
 1016 Gur greywackes). These interludes may have been peri-
 1017 ods of inactivity or alternatively when phreatomagmatic
 1018 activity was too deep for debris jets to breach the
 1019 surface and eject material. The occurrence of lithic
 1020 clasts within this deposit marks the onset of country
 1021 rock brecciation and diatreme-forming phreatomagmatic
 1022 activity.

A minor late phase of magmatic activity, largely affect- 1023
 ing the lower parts of the diatremes, was most likely 1024
 associated with emergence and subsequent drying out of 1025
 the maar-diatreme system. Here, the presence of lapilli 1026
 of apparent magmatic or low water/magma origin (e.g. 1027
 ‘raggy’ and globular lapilli) suggests the diatremes lie 1028
 somewhere between the two end members of magmatic and 1029
 phreatomagmatic activity. 1030

Our observations of diatreme architecture coupled with 1031
 their extra-crater deposits, reveal a complicated eruption 1032
 chronology of maar-diatremes initially in a submarine 1033
 environment, which will have implications for the study of 1034
 other volcanic systems. 1035

Acknowledgments We would like to thank Teck Ireland Ltd. 1036
 for funding this study. We would particularly like to thank the 1037
 Teck team at Limerick, including Ashley Murray, Jim McCusker 1038
 and Chris Reed for their helpful discussions and knowledge of 1039
 the country rock stratigraphy and to the support staff for help- 1040
 ing move many heavy boxes of core. We would also like 1041
 to thank the editor, James White and the reviewers of this 1042
 manuscript including an anonymous reviewer, Richard Brown and 1043
 Pierre-Simon Ross for their helpful and detailed comments and 1044
 suggestions. 1045

References 1046

Allen SR, Fiske RS, Cashman KV (2008) Quenching of steam-charged 1047
 pumice: Implications for submarine pyroclastic volcanism. *Earth* 1048
Planet Sci Lett 274(1):40–49 1049
 Aranda-Gómez J, Luhr JF (1996) Origin of the Joya Honda maar, San 1050
 Luis Potosi, Mexico. *J Volcanol Geotherm Res* 74:1–18 1051
 Ashby DF (1939) The geological succession and petrology of the 1052
 Lower Carboniferous volcanic area of Co. Limerick *Proc Geol* 1053
Assoc 50:324–330 1054
 Banks DA, Boyce AJ, Samson IM (2002) Constraints on the 1055
 origins of fluids forming Irish Zn-Pb-Ba deposits: Evidence 1056
 from the composition of fluid inclusions. *Econ Geol* 97: 1057
 471–480 1058
 Brand BD, Clarke AB (2009) The architecture, eruptive history, and 1059
 evolution of the Table Rock Complex, Oregon: from a Surt- 1060
 seyan to an energetic maar eruption. *Volcanol Geotherm Res* 1061
 180:203–224 1062
 Branney MJ, Kokelaar P (2002) *Pyroclastic density of ignimbrites.* 1063
 Geological Society, London. Special Publications No 27 1064
 Brown RJ, Field M, Gernon TM, Gilbertson M, Sparks RSJ (2008b) 1065
 Problems with an in-vent column collapse model for the emplace- 1066
 ment of massive volcanoclastic kimberlite. A discussion of ‘In-vent 1067
 column collapse as an alternative model for massive volcanoclas- 1068
 tic kimberlite emplacement: an example from the Fox kimberlite, 1069
 Ekati Diamond Mine, NWT, Canada’ by Porritt et al. [*J Vol-* 1070
canol Geotherm Res 174, 90–102]. *J Volcanol Geotherm Res* 1071
 178:847–850 1072
 Brown RJ, Gernon T, Stiefenhofer J, Field M (2008a) Geo- 1073
 logical constraints on the eruption of the Jwaneng Centre 1074
 kimberlite pipe, Botswana. *J Volcanol Geotherm Res* 174: 1075
 195–208 1076
 Calvari S, Tanner LH (2011) The Miocene Costa Giardini dia- 1077
 treme, Iblean Mountains, southern Italy: Model for maar-diatreme 1078

1079 formation on a submerged carbonate platform. *Bull Volcanol* 1143
 1080 73:557–576 1144
 1081 Cas RAF, Wright JV (1988) Volcanic successions: Modern and 1145
 1082 ancient, 2nd edn. Unwin Hyman Ltd, London 1146
 1083 Cas RAF, Porritt L, Pittari A, Hayman P (2008) A new 1147
 1084 approach to kimberlite facies terminology using a revised gen- 1148
 1085 eral approach to the nomenclature of all volcanic rocks and 1149
 1086 deposits: Descriptive to genetic. *J Volcanol Geotherm Res* 174: 1150
 1087 226–240 1151
 1088 Cas RAF, Wright JV (1991) Subaqueous pyroclastic flows and ign- 1152
 1089 imbrites: an assessment. *Bull Volcanol* 53:357–380 1153
 1090 Davies AGS, Cooke DR, Gemmell JB, Simpson KA (2008) Dia- 1154
 1091 treme breccias at the Kelian gold mine, Kalimantan, Indone- 1155
 1092 sia: precursors to epithermal gold mineralization. *Econ Geol* 1156
 1093 103:689–716 1157
 1094 Delpit S, Ross P-S, Hearn BC (2014) Deep-bedded ultramafic dia- 1158
 1095 tremes in the Missouri River Breaks volcanic field, Montana, 1159
 1096 USA: 1 km of syn-eruptive subsidence. *Bull Volcanol* 76:832–854 1160
 1097 Field M, Scott Smith B (1999) Contrasting geology and near-surface 1161
 1098 emplacement of kimberlite pipes in Southern Africa and Canada. 1162
 1099 In: Gurney JJ, Gurney ML, Pascoe MD, Richardson SH (eds) Pro- 1163
 1100 ceedings of the VII th International Kimberlite Conference, vol 1, 1164
 1101 pp 214–237 1165
 1102 Fisher RV (1961) Proposed classification of volcanoclastic sediments 1166
 1103 and rocks. *Geol Soc Am Bull* 72:1409–1414 1167
 1104 Fisher RV, Waters AC (1970) Base surge bed forms in maar volcanoes. 1168
 1105 *Am J Sci* 268:157–180 1169
 1106 Fisher RV (1984) Pyroclastic rocks. Springer-Verlag, Berlin Heidel- 1170
 1107 berg 86:937–938 1171
 1108 Fiske RS, Cashman KV, Shibata A, Watanabe K (1998) Tephra disper- 1172
 1109 sal from Myojinsho, Japan, during its shallow submarine eruption 1173
 1110 of 1952-1953. *Bull Volcanol* 59:262–275 1174
 1111 Francis EH (1970) Bedding in Scottish (Fifeshire) tuff-pipes and its 1175
 1112 relevance to maars and calderas. *Bull Volcanol* 34:697–712 1176
 1113 Gallagher SJ, Somerville ID (2003) Lower Carboniferous (Late 1177
 1114 Viséan) platform development and cyclicity in Southern Ireland: 1178
 1115 foraminiferal biofacies and lithofacies evidence. *Rivista Italiana di* 1179
 1116 *Paleontologia e Stratigrafia* 109:159–171 1180
 1117 Geikie A (1897) The ancient volcanoes of Great Britain. Vol. 1 and 2. 1181
 1118 McMilland & Co. 1182
 1119 Gernon T, Brown RJ, Tait MA, Hincks TK (2012) The origin of 1183
 1120 pelletal lapilli in explosive kimberlite eruptions. *Nat Commun* 1184
 1121 3:1–7 1185
 1122 Gernon TM, Field M, Sparks RSJ (2009a) Depositional processes 1186
 1123 in a kimberlite crater: the Upper Cretaceous Orapa South Pipe 1187
 1124 (Botswana). *Sedimentology* 56:623–643 1188
 1125 Gernon TM, Gilbertson MA, Sparks RSJ, Field M (2008) Gas- 1189
 1126 fluidisation in an experimental tapered bed: Insights into pro- 1190
 1127 cesses in diverging volcanic conduits. *J Volcanol Geotherm Res* 1191
 1128 174:49–56 1192
 1129 Gernon TM, Gilbertson MA, Sparks RSJ, Field M (2009b) The 1193
 1130 role of gas-fluidisation in the formation of massive volcanoclastic 1194
 1131 kimberlite. *Lithos* 112, Supplement 1:439–451 1195
 1132 Gernon TM, Upton BGI, Hincks TK (2013) Eruptive history of 1196
 1133 an alkali basaltic diatreme from Elie Ness, Fife, Scotland. *Bull* 1197
 1134 *Volcanol* 75:704–724 1198
 1135 Graetinger AH, Valentine GA, Sonder I, Ross P-S, White JDL, Tad- 1199
 1136 deucci J (2014) Maar-diatreme geometry and deposits: Subsurface 1200
 1137 blast experiments with variable explosion depth. *Geochemistry,* 1201
 1138 *Geophysics, Geosystems* 15:740–764 1202
 1139 Gregg TKP, Fink JH (1995) Quantification of submarine lava-flow 1203
 1140 morphology through analog experiments. *Geology* 23:73–76 1204
 1141 Griffiths RW (1992) Solidification and morphology of submarine 1205
 1142 lavas: a dependence on extrusion rate. *J Geophys Res* 97:729–737 1206
 Hawthorne JB (1975) Model of a kimberlite pipe. *Phys Chem Earth* 1143
 9:1–15 1144
 Heiken G (1972) An atlas of volcanic ash. *Smithson Contrib Earth Sci* 1145
 12:1–101 1146
 Hitzman MW (1995) Geological setting of the Irish Zn-Pb-(Ba-Ag) 1147
 Orefield. In: Anderson K, Ashton J, Earls G, Hitzman M, Tear 1148
 S (eds) *Irish Carbonate-hosted Zn-Pb Deposits*. Vol. 21 of Guide- 1149
 book Series. Society of Economic Geologists, pp 3–24 1150
 Hitzman MW, Beatty DW (1996) The Irish Zn-Pb-(Ba) Orefield. *Soc* 1151
Econ Geol Spec Publ 4:112–143 1152
 Hitzman MW, Redmond PB, Beatty DW (2002) The carbonate-hosted 1153
 Lisheen Zn-Pb-Ag deposit, County Tipperary, Ireland. *Econ Geol* 1154
 97:1627–1655 1155
 Holland CH, Sanders IS (2009) *The Geology of Ireland*, 2nd edn. 1156
 Dunedin Academic Press 1157
 Houghton BF, Wilson CJN (1989) A vesicularity index for pyroclastic 1158
 deposits. *Bull Volcanol* 51:451–462 1159
 Houghton BF, Smith RT (1993) Recycling of magmatic clasts dur- 1160
 ing explosive eruptions: estimating the true juvenile content of 1161
 phreatomagmatic volcanic deposits. *Bull Volcanol* 55:414–420 1162
 Houghton BF, Wilson CJN, Smith IEM (1999) Shallow-seated con- 1163
 trols on styles of explosive basaltic volcanism: a case study from 1164
 New Zealand. *Journal of Volcanology and Geothermal Research* 1165
 91:97–120 1166
 Humphris SE, Thompson G (1978) Hydrothermal alteration of 1167
 oceanic basalts by seawater. *Geochimica et Cosmochimica Acta* 1168
 42:107–125 1169
 Ingram RL (1964) Terminology for the thickness of stratification and 1170
 parting units in sedimentary units. *Bull Geol Society of America* 1171
 86:937–938 1172
 Kneller B, Branney MJ (1995) Sustained high-density turbidity cur- 1173
 rents and the deposition of thick massive sands. *Sedimentology* 1174
 42:607–616 1175
 Kokelaar BP (1983) The mechanism of Surtseyan volcanism. *J Geol* 1176
Society of London 140:939–944 1177
 Kokelaar BP (1986) Magma-water interactions in subaqueous and 1178
 emergent basaltic volcanism. *Bull Volcanol* 48:275–289 1179
 Kurszlaukis S, Barnett W (2003) Volcanological and structural aspects 1180
 of the Venetia kimberlite cluster - as case study of South 1181
 African kimberlite maar-diatreme volcanoes. *South African J Geol* 1182
 106:145–172 1183
 Kurszlaukis S, Franz L, Lorenz V (1998) On the volcanology of 1184
 the Gibeon kimberlite field, Namibia. *J Volcanol Geother Res* 1185
 84:257–272 1186
 Kurszlaukis S, Lorenz V (1997) Volcanological features of a low- 1187
 viscosity melt: the carbonatitic Gross Brukkaros volcanic field, 1188
 Namibia. *Bull Volcanol* 58:421–431 1189
 Leahy K (1997) Discrimination of reworked pyroclastics from primary 1190
 tephra-fall tuffs: a case study using kimberlites of Fort a la Corne, 1191
 Saskatchewan, Canada. *Bull Volcanol* 59:65–71 1192
 Lees A, Miller J (1985) Facies variation in Waulsortian buildups. part 1193
 2; Mid-Dinantian buildups from Europe and North America. *Geol* 1194
J 20:159–180 1195
 Lefebvre NS, White JDL, Kjarsgaard BA (2013) Unbedded diatreme 1196
 deposits reveal maar-diatreme-forming eruptive processes: Stand- 1197
 ing Rocks West, Hopi Buttes, Navajo Nation, USA. *Bull Volcanol* 1198
 75:739–756 1199
 Lloyd FE, Stoppa F (2003) Pelletal lapilli in diatremes—some inspira- 1200
 tion from the old masters. *GeoLines* 15:65–71 1201
 Lorenz V (1975) Formation of phreatomagmatic maar-diatreme volca- 1202
 noes and its relevance to kimberlite diatremes. *Phys Chem Earth* 1203
 9:17–27 1204
 Lorenz V (1985) Maars and diatremes of phreatomagmatic origin: a 1205
 review. *Transac Geol Society of South Africa* 88:459–470 1206

- 1207 Lorenz V (1986) On the growth of maars and diatremes and its
1208 relevance to the formation of tuff rings. *Bull Volcanol* 48:265–274
1209 Lorenz V (2003) Maar-diatreme volcanoes, their formation, and their
1210 setting in hard-rock or soft-rock environments. *Geolines* 15:
1211 72–83
1212 Lorenz V (2007) Syn- and posteruptive hazards of maar-diatreme
1213 volcanoes. *J Volcanol Geother Res* 159:285–312
1214 Lorenz V, Kurszlaukis S (2007) Root zone processes in the
1215 phreatomagmatic pipe emplacement model and consequences for
1216 the evolution of maar–diatreme volcanoes. *J Volcanol Geother Res*
1217 159:4–32
1218 Lorenz V, Zimanowski B, Buettner R (2002) On the formation of
1219 deep-seated subterranean peperite-like magma-sediment mixtures.
1220 *J Volcanol Geother Res* 114:107–118
1221 MacLean WH (1980) Mass change calculations in altered rock series.
1222 *Miner Deposita* 25:44–49
1223 Mangan MT, Cashman KV (1996) The structure of basaltic scoria
1224 and reticulite and inferences for vesiculation, foam formation,
1225 and fragmentation in lava fountains. *J Volcanol Geother Res*
1226 73:1–18
1227 Mattsson HB (2010) Textural variation in juvenile pyroclasts from
1228 an emergent, Surtseyan-type, volcanic eruption: the Capelas
1229 tuff cone, Sao Miguel (Azores). *J Volcanol Geother Res*
1230 189:81–91
1231 Mattsson HB, Hoskuldsson A, Hand S (2005) Crustal xenoliths in the
1232 6220 BP saefell tuff-cone, south Iceland: Evidence for a deep,
1233 diatreme-forming, Surtseyan eruption. *J Volcanol Geother Res*
1234 145:234–248
1235 McClintock M, White JDL (2006) Large phreatomagmatic vent com-
1236 plex at Coombs Hills, Antarctica: wet, explosive initiation of
1237 flood basalt volcanism in the Ferrar-Karoo LIP. *Bull Volcanol*
1238 68:215–239
1239 McCusker J, Reed C (2013) The role of intrusions in the formation of
1240 Irish-type mineralisation. *Miner Deposita* 48:687–695
1241 Mitchell RH (1990) Kimberlites and lamproites: Primary sources of
1242 diamond. *Geoscience Canada* 18:1–16
1243 Moore JG (1985) Structure and eruptive mechanisms at Surtsey Vol-
1244 cano, Iceland. *Geol Mag* 122:649–661
1245 Mueller W, White JDL (1992) Felsic fire-fountaining beneath Archean
1246 seas: Pyroclastic deposits of the 2730 Ma Hunter Mine Group,
1247 Quebec, Canada. *J Volcanol Geother Res* 54:117–134
1248 Mundula F, Cioni R, Funedda A, Leone F (2013) Lithofacies char-
1249 acteristics of diatreme deposits: Examples from a basaltic volcanic
1250 field of SW Sardinia (Italy). *J Volcanol Geother Res* 255:1–14
1251 Nemeč W, Steel RJ (1984) Alluvial and coastal conglomerates:
1252 their significant features and some comments on gravelly mass-
1253 flow deposits. In: *Sedimentology of Gravels and Conglomerates*.
1254 Vol. 10. Canadian Society of Petroleum Geology Memoirs,
1255 pp 1–31
1256 Nemeth K, Martin U, Harangi S (2001) Miocene phreatomagmatic
1257 volcanism at Tihany (Pannonian Basin, Hungary). *J Volcanol*
1258 *Geother Res* 111:111–135
1259 Pittari A, Cas RAF, Lefebvre NS, Robey J, Kurszlaukis S, Webb
1260 K (2008) Eruption processes and facies architecture of the
1261 Orion Central kimberlite volcanic complex, Fort á la Corne,
1262 Saskatchewan; kimberlite mass flow deposits in a sedimentary
1263 basin. *J Volcanol Geother Res* 174:152–170
1264 Porritt LA, Cas RAF, Crawford BB (2008) In-vent column col-
1265 lapse as an alternative model for massive volcanoclastic kimberlite
1266 emplacement: an example from the Fox kimberlite, Ekati Dia-
1267 mond Mine, NWT, Canada. *J Volcanol Geother Res* 174:90–
1268 102
1269 Redmond PB (2010) The Limerick Basin: an important emerging
1270 subdistrict of the Irish Zn-Pb orefield. *Soc Econ Geol Newsl*
1271 82:21–25
Riding R (1975) Girvanella and other algae as depth indicators. *Lethaia* 8:173–179
Rollinson H (1993) Using geochemical data: Evaluation, presentation, interpretation. Pearson Education Limited
Ross P-S, White JDL (2006) Debris jets in continental phreatomagmatic volcanoes: a field study of their subterranean deposits in the Coombs Hills vent complex, Antarctica. *J Volcanol Geother Res* 149:62–84
Ross P-S, White JDL (2012) Quantification of vesicle characteristics in some diatreme-filling deposits, and the explosivity levels of magma-water interactions within diatremes. *J Volcanol Geother Res* 245:55–67
Ross P-S, White J, Zimanowski B, Büttner R (2008) Rapid injection of particles and gas into non-fluidized granular material, and some volcanological implications. *Bull Volcanol* 70:1151–1168
Ross P-S, White J, Zimanowski B, Büttner R (2008) Multi-phase flow above explosion sites in debris-filled volcanic vents: Insights from analogue experiments. *J Volcanol Geother Res* 178:104–112
Rottas KM, Houghton BF (2012) Structure, stratigraphy, and eruption dynamics of a young tuff ring: Hanauma Bay, O’ahu, Hawai’i. *Bull Volcanol* 74:1683–1697
Sahagian DL, Proussevitch AA (1998) 3D particle size distributions from 2D observations: Stereology for natural applications. *J Volcanol Geother Res* 84:173–196
Seyfried WE, Mottl MJ (1982) Hydrothermal alteration of basalt by seawater under seawater-dominated conditions. *Geochimica et Cosmochimica Acta* 46:985–1002
Shea T, Houghton BF, Gurioli L, Cashman KV, Hammer JE, Hobden, B J (2010) Textural studies of vesicles in volcanic rocks: an integrated methodology. *J Volcanol Geother Res* 190:271–289
Shimano T, Nakada S (2006) Vesiculation path of ascending magma in the 1983 and the 2000 eruptions of Miyakejima volcano, Japan. *Bull Volcanol* 68:549–566
Sohn YK (1996) Hydrovolcanic processes forming basaltic tuff rings and cones on Cheju Island, Korea. *Geol Soc Am Bull* 108:1199–1211
Somerville ID, Strogen P (1992) Ramp sedimentation in the Dinantian limestones of the Shannon Trough, Co. Limerick, Ireland. *Sedimentary Geol* 79:59–75
Somerville ID, Strogen P, Jones GL (1992) Biostratigraphy of Dinantian limestones and associated volcanic rocks in the Limerick Syncline, Ireland. *Geol J* 27:201–220
Sottili G, Taddeucci J, Palladino DM, Gaeta M, Scarlato P, Ventura G (2009) Sub-surface dynamics and eruptive styles of maars in the Colli Albani Volcanic District, Central Italy. *J Volcanol Geother Res* 180:189–202
Sparks RSJ, Baker L, Brown RJ, Field M, Schumacher J, Stripp G, Walters A (2006) Dynamical constraints on kimberlite volcanism. *J Volcanol Geother Res* 155:18–48
Strogen P (1983) The geology of the volcanic rocks of southeast County Limerick. Ph.D. thesis. University College Dublin
Strogen P (1988) The carboniferous lithostratigraphy of southeast County Limerick, Ireland, and the origin of the Shannon trough. *Geol J* 23:121–137
Strogen P, Somerville ID, Pickard NAH, Jones GL, Fleming M (1996) Controls on ramp, platform and basinal sedimentation in the Dinantian of the Dublin Basin and Shannon Trough, Ireland. *Geological Society, London. Spec Publ* 107:263–279
Timmerman MJ (2004) Timing, geodynamic setting and character of Permo-Carboniferous magmatism in the foreland of the Variscan Orogen, NW Europe. In: Wilson M, Neumann ER, Davies GR, Timmerman MJ, Heeremans M, Larsen BT (eds)

1336	Permo-Carboniferous Magmatism And Rifting in Europe, vol 223. Geol Soc, London, pp 41–74	White JDL, Houghton BF (2006) Primary volcanoclastic rocks. <i>Geology</i> 34:677	1362
1337			1363
1338	Tsukui M, Suzuki Y (1995) Vesiculation of basaltic magma: Magmatic versus phreatomagmatic eruption in 1983 eruption of Miyakejima. <i>Volcanol Soc Japan</i> 40:395–399	White JDL, Ross P-S (2011) Maar-diatreme volcanoes: a review. <i>J Volcanol Geother Res</i> 201:1–29	1364
1339			1365
1340	Utzmann A, Hansteen TH, Schminke HU (2002) Trace element mobility during sub-seafloor alteration of basaltic glass from Ocean Drilling Program site 953 (off Gran Canaria). <i>Int J Earth Sci</i> 91:661–679	Wilkinson JJ, Eyre SL, Boyce AJ (2005) Ore-forming processes in Irish-Type carbonate-hosted Zn-Pb deposits: Evidence from mineralogy, chemistry, and isotopic composition of sulfides at the Lisheen Mine. <i>Econ Geol</i> 100: 63–86	1366
1341			1367
1342	Valentine GA (2012) Shallow plumbing systems for small-volume basaltic volcanoes, 2: evidence from crustal xenoliths at scoria cones and maars. <i>J Volcanol Geother Res</i> 223:47–63	Wilson B, Neumann ER, Davies GR, Timmerman MJ, Heeremans M, Larsen BT (2004) Permo-carboniferous magmatism and rifting in Europe. Special Publications. Geological Society of London, London	1368
1343			1369
1344	Valentine GA, White JD (2012) Revised conceptual model for maar-diatremes: Subsurface processes, energetics, and eruptive products. <i>Geology</i> 40:1111–1114	Wohletz KH, McQueen RC (1984) Experimental studies of hydro-magmatic volcanism. In: Boyd FR, Boettcher AL, Company (eds) Explosive volcanism: Inception, evolution, and hazards. National Academy Press, pp 158–170	1370
1345			1371
1346	Walters AL, Phillips JC, Brown RJ, Field M, Gernon T, Stripp G, Sparks RSJ (2006) The role of fluidisation in the formation of volcanoclastic kimberlite: Grain size observations and experimental investigation. <i>J Volcanol Geother Res</i> 155:119–137	Wood A (1957) The type-species of the genus <i>Girvanella</i> (calcareous algae). <i>Palaeontology</i> 1:22–28	1372
1347			1373
1348	White JDL (1991) Maar-diatreme phreatomagmatism at Hopi Buttes, Navajo Nation (Arizona), USA. <i>Bull Volcanol</i> 53:239–258	Woodcock NH, Strachan R (2000) Geological history of Britain and Ireland. Blackwell Science, Oxford	1374
1349			1375
1350	White JDL (1996) Pre-emergent construction of a lacustrine basaltic volcano, Pahvant Butte, Utah USA. <i>Bull Volcanol</i> 58:249–262	Zhou Y, Bohor BF, Ren Y (2000) Trace element geochemistry of altered volcanic ash layers (tonsteins) in Late Permian coal-bearing formations of eastern Yunnan and western Guizhou Provinces, China. <i>Int J Coal Geol</i> 44: 305–324	1376
1351			1377
1352	White JDL (2000) Subaqueous eruption-fed density currents and their deposits. <i>Precambrian Res</i> 101:87–109		1378
1353			1379
1354			1380
1355			1381
1356			1382
1357			1383
1358			1384
1359			1385
1360			1386
1361			1387

UNCORRECTED PROOF

AUTHOR QUERIES

AUTHOR PLEASE ANSWER ALL QUERIES:

- Q1.** Please check the affiliation if it was captured and presented correctly.
- Q2.** Keywords are required, please check if the suggested keywords 'Raggy, Maar-diatremes, Lower Carboniferous Period' are correct.